Trinity River Juvenile Salmonid Habitat Synthesis: Physical Habitat Capacity at the Restoration Site and Reach Scale

August 2022

Emily Cooper-Hertel, Dave Gaeuman, Kyle De Juilio, Aaron Martin
Yurok Tribe
Yurok Tribal Fisheries Program
Klamath, California 95548
(530) 430-1350

Josh Boyce, Damon Goodman, Nicholas Som
U.S. Fish and Wildlife Service
Arcata Fish and Wildlife Office
1655 Heindon Road, Arcata, California 95521
(707) 822-7201

Justin Alvarez
Hoopa Valley Tribe
Hoopa Valley Tribal Fisheries Department
Hoopa, California 95546
(530) 625-4267

Trinity River Juvenile Salmonid Habitat Synthesis: Physical Habitat Capacity at the Restoration Site and Reach Scale

Emily J. Cooper-Hertel, David Gaeuman, Kyle DeJuilio, Aaron Martin, Josh Boyce, Damon Goodman, Nicholas Som, and Justin Alvarez

Abstract

The TRRP aims to restore salmonid habitat for population recovery through mechanical restoration and flow management targeted in the 64-km reach below Lewiston Dam, known as the restoration reach. Restoration strategies are intended to evolve through adaptive management regarding habitat assessment, restoration action, and rehabilitation effectiveness monitoring. This report synthesizes data collected in the Trinity River restoration reach for flows, physical terrain, hydraulics, and fish distribution. These data informed the development of a spatially explicit, flow specific hydrodynamic fish capacity model we used to assess TRRP's efforts to rehabilitate habitat for juvenile Chinook Salmon (*Oncorhynchus tshawytscha*). Rehabilitated areas had greater capacity than non-rehabilitated areas in four out of seven hydrologically distinct sub-reaches. Evaluation of capacity-flow relationships between sub-reaches and rehabilitation sites showed that capacity was generally greater in upstream areas compared to downstream areas. Reach-scale fry and presmolt capacity was positively related to topographic complexity within the active channel and to wetted width. We concluded that confined wetted width limits physical capacity in downstream sub-reaches, likely due to planform setting affected by mine tailings and subsequent incision. Under current management, winter baseflow limits capacity during 70% of the rearing period, especially for the fry life stage, and we found that fry capacity tends to be limited over a wider and more frequent range of flows in downstream reaches. Throughout the entire restoration reach, increasing baseflow to 14.2 m^3/s decreases capacity by 7%, but increasing baseflow to 28.3 m^3/s, 42.5 m^3/s or 56.7 m^3/s would increase capacity by 2%, 18% or 25%, respectively, during the rearing period. We recommend rehabilitation efforts prioritize increasing topographic complexity within the active channel and designing features that increase wetted width at discharges that occur for long durations during the critical rearing period to facilitate juvenile salmonid rearing. We also recommend that alternative flow management during the critical rearing period be evaluated for its role in alleviating habitat bottlenecks for fry and presmolt life stages in winter and spring.

Table of Contents

List of Figures

List of Tables

Introduction: Fish habitat

Hydrologic regime on the Trinity River from past to present

Trinity River hydrology historically had a winter rain and low volume snowmelt driven hydrograph (USFWS and HVT 1999, Lane et al. 2017). The unregulated Trinity River flow data from USGS gage near Lewiston (11525500) during water years (WY) prior to WY1961 show flows increasing in late October to November, reaching peak magnitudes during winter and spring months, beginning hydrograph recession around mid-May, and reaching seasonal low-flows in September. Understanding pre-regulation flow duration, frequency, magnitude, and timing is important for assessing present-day habitat, flow management, and river restoration goals.

Dam and diversion regulation on the Trinity River dampened volume and variability of flow and bedload downstream of Lewiston Dam, resulting in a smaller, uniform mainstem channel (Barinaga et al. 1996) in what previously was a seasonally dynamic, alluvial, and disturbance-dependent riverine habitat. Flow management, in combination with legacy hydraulic mining impacts that left enormous amounts of sediment in the valley bottom, resulted in incision and entrenchment followed by development of highly vegetated berms along river channel margins (USFWS and HVT 1999). The result was a straight channel with reduced variation in channel bed elevation between riffles and pools and little opportunity for lateral meandering or floodplain inundation. These impacts were primarily observed in the 64-km reach directly downstream of Lewiston Dam, commonly referred to as the restoration reach.

In 1961, the Trinity River Division (TRD) began dam and diversion operations authorized by the United States Congress 1955 Trinity River Act (USHR 1955), allowing up to 90% of the Trinity River's mean annual flow at Lewiston to be diverted to the Central Valley Project (CVP) water allocations (USFWS and HVT 1999). Management of the newly regulated Trinity River downstream of Lewiston Dam was informed with minimum environmental flow recommendations by the California Department of Fish and Game at 4.2 (m^3/s) year-round, except when safety of dam or reservoir management required otherwise (USFWS and CDFG 1956). TRD dam and diversion operations blocked access for fish to 24% (1,862 km^2) of the Trinity River's total basin area (7,692 km^2) upstream of Lewiston Dam, while also degrading remaining habitats for native fish and aquatic species downstream. Population declines of salmon, trout, and other native aquatic species quickly followed. Native fish are keystone species of a healthy ecosystem, and their populations are important cultural subsistence resources for Native American Tribes in the Klamath Basin since time immemorial. After decades of documented downstream impacts from altered flow and sediment regimes in a river ecosystem which evolved with annual variations in flood disturbance (Barinaga et al. 1996, McBain & Trush 1997, USFWS and HVT 1999), a Record of Decision (ROD) was signed in 2000 to improve instream flows for maintaining fluvial geomorphic processes and restoring habitat for native anadromous fish undergoing massive population declines (USDI 2000).

Changes in flow release strategy were enacted over the following decades. The ROD instituted flow releases from Lewiston Dam each year beginning in mid-April based on the water year forecast, which determines the volume for spring flow releases. While flow release strategies are a major management action of the ROD, the other side of the coin lies within mechanical channel rehabilitation. Both channel rehabilitation and flow management efforts coincide; evaluation of their accompaniment is therefore important when assessing TRRP actions.

History of restoration on Trinity River

Prior to the signing of the ROD in 2000 there were efforts to restore the Trinity River. As early as 1970, restoration actions associated with maintenance of spawning riffles and deep pools through mechanical means and flushing flows were being pursued (Krause 2012). Efforts continued in the 1980's with side channel construction (USFWS 1989; USBR 1984) and in the 1990's with 'feathered edge' projects which attempted to address the confinement of the channel by the riparian berm (USFWS and HVT 1999). The Trinity River Flow Evaluation (TRFE) was ordered by the secretary of Department of Interior in the late 1980's and laid the scientific foundation that underlies the ROD.

The TRFE from USFWS and HVT (1999) and ROD identified 47 potential channel rehabilitation sites and three potential side channels. The TRFE and ROD strategy for habitat rehabilitation was to foster a scaled down, dynamic alluvial channel that ROD flow and sediment management activities could maintain and evolve (HVT et al. 2011). However, because those objectives could not be achieved by ROD flows alone, mechanical channel modifications were required.

Channel restoration activities under direction of the TRRP began in 2005 with the Hocker Flat rehabilitation site. Four more sites were constructed in 2006 (Conner Creek, Elkhorn, Valdor and Pear Tree) in the lower portion of the restoration reach, downstream of Canyon Creek where higher flows were expected to be more prevalent. The restoration approach for these five sites was essentially berm and vegetation removal to initiate river processes that were expected to increase channel complexity and instream habitat. Little to no instream work was performed during construction of these first five sites. These limited actions resulted in relatively small contributions of salmonid rearing habitat (Goodman et al. 2010; Alvarez et al. 2015) at these sites even following large flow events greater than 566 m^3/s, such as the floods of December 2005 (USGS gage 11526400).

Beginning in 2008, a new design and construction approach was implemented that included large wood placement, main channel realignment, and extensive off-channel habitat creation and enhancement including alcoves, side channels, ponds, and floodplains (Alvarez et al 2015). A wide variety of these types of features were created at 18 sites, through the 2016 Bucktail site revisit, captured by data analyzed in this report. Since 2014, construction strategy included more emphasis on lowered floodplains and ponds in addition to approaches since 2008 such as wood placement, channel realignment, and side channels. Since 2016, site construction

has continued at four projects located upstream of Junction City (Dutch Creek, Deep Gulch, Sheridan Creek, and Chapman Ranch). Sites occurring since 2016 are not captured by the data in this report, but have continued construction strategies since 2014 described previously. Current designs for projects to be implemented after the completion of this report (Oregon Gulch and Lower Connor Creek) include even more extensive floodplain lowering attempting to achieve valley wide restoration where opportunities permit (Yurok Tribe 2021).

History of habitat measurement and evaluation on Trinity River

To assess changes in physical habitat, it must be defined and quantified. The first thorough written characterization of Trinity River fish distribution and habitats was completed in 1950, by the USFWS (Moffett and Smith 1950) to inform plans for development of the Trinity River's water resources. This study detailed the seasonality with which species utilized reaches of the unregulated Trinity River for life history needs. It also summarized impacts, as they were understood, of two plans to develop the Trinity River's water resources through impoundment and diversion.

Salmonid habitat described by Moffett and Smith (1950) was characterized by the areas in which adult salmonids spawned in fall and winter. There was documentation of the same areas being used by migrating and rearing juveniles and migrating and holding adults. Chinook Salmon were documented to use the mainstem Trinity River between the confluence with North Fork Trinity River and the confluence with Ramshorn Creek, as well as three major tributaries (Stuart's Fork identified as the most important, while the other two tributaries were not clearly identified). Other salmonid species were described as primarily using tributary habitats. Water temperature was noted as an important component of habitat that limited migratory behaviors and restricted holding and rearing to cold water refuge during late summer (Moffett and Smith 1950). The plan to develop the Trinity's water resources that was eventually implemented included Trinity and Lewiston Dams and blocked access to 50% of existing Chinook Salmon spawning habitat (Moffett and Smith 1950). An alternative plan that included a downstream dam located near the confluence with Brown's Creek and would have caused more severe impacts to habitat by rendering 82% of Chinook Salmon spawning habitat unusable.

Development of the water resources of the Trinity River came to pass with the construction of the TRD of the CVP in the early to mid-1960's. Mitigation recommendations provided by Moffett and Smith (1950) were selectively implemented, with artificial propagation, 4.2 m^3/s minimum discharge, and inaction on the Brown's Creek Dam being the most significant. The 50% reduction in available habitat was only one impact resulting from impoundment and streamflow regulation. It would later become understood and documented that these actions severely degraded the remaining habitat below Lewiston Dam through channelization and coarsening of bed and banks, which were subsequently densely colonized by riparian vegetation (USFWS and HVT 1999). Additional documented impacts to habitat include changes to water temperature and sequestration of sediment (USFWS and HVT 1999) and large woody debris (HVT et al. 2011).

Starting in the 1980's and 1990's concerns for temperature requirements of holding adult salmonids prior to and during spawning (SWRCB 1990) and for the physical habitat required for juvenile salmonids to rear prior to their seaward migration became more prevalent among managers. These concerns resulted in extensive review of juvenile salmonid rearing habitat needs (Hampton 1988 and 1997). Efforts designed to characterize preferred habitat of rearing juveniles relied on direct observation in various habitats and resulted in a detailed understanding of the depths and velocities that juvenile salmonids select for rearing purposes, referred to as habitat suitability criteria (HSC). These HSC allowed for habitat to be measured and quantified, resulting in many efforts to physically map and model available juvenile rearing habitat.

Efforts to use 2-dimensial (2-D) hydrodynamic models to predict physical habitat quality and quantity were attempted as early as 1999 (Gallagher 1999(a)). These modeling efforts applied HSC to outputs and summarized results as weighted usable area (WUA), a spatial summation of habitat quantity and quality. Difficulty and expense of collecting data required for 2-D modeling with existing technology was prohibitive and led to most applications, and particularly those that covered a relatively large geographic area being conducted with 1-D modeling platforms (Aceituno et al. 1997, USFWS and HVT 1999). Other efforts relied on direct measurement applied to HSC, but were limited in geographic scope and discharges that could be evaluated due to intensity of the effort required to collect the necessary census data (Gallagher 1999(b)). Many efforts to characterize physical juvenile salmonid rearing habitat identified a 'habitat dip' or reduced habitat availability at moderate discharges when flows are confined within the channel banks and velocities increase (USFWS and HVT 1999). These findings resulted in the 300 cfs winter baseflow prescription provided by the ROD, for the stated objective of providing rearing and spawning habitat.

In 2007 juvenile rearing habitat monitoring was re-invigorated to assess how both flow and channel rehabilitation efforts conducted by the TRRP were affecting habitat quality and quantity. Another set of direct observations were used to generate updated HSC, and study sites along the river were measured and mapped (Chamberlin et al. 2007). The practice of measuring and mapping habitat based on HSC thresholds continued until 2017 and the methods were refined. Methods used over most of that time are detailed in Goodman et al. 2014. The rejuvenated effort to monitor physical habitat was intended to be more inclusive of other salmonid life stages, aquatic species, riparian plants, and geomorphic change (HVTFD and McBain & Trush 2012, Alvarez et al. 2015(a)). However, due to differing data collection methods and timelines for reporting, this broader effort, dubbed the Integrated Habitat Assessment Plan (IHAP), was short lived.

The physical habitat mapping methods described above separated habitat into guilds that could be summed over area for different life stages and suitability (Goodman et al. 2014). The methods were efficient and repeatable, resulting in assessments of systemic habitat availability at an index flow (Alvarez et al. 2013, Boyce et al. 2018, Goodman et al. 2012, Goodman et al. 2016), and census at a range of flows at channel rehabilitation sites in their pre-construction, post constriction, and evolved states (Boyce et al. 2020, De Juilio et al. 2014, Goodman et al. 2010, Martin et al. 2012, Martin et al. 2013). The methods allowed for relatively quick data processing

and presentation of results and benefited project designers with timely feedback on recently constructed projects. However, data collection for this assessment method required flows to be manipulated to allow for mapping to occur at relatively stable flow over an extended period (weeks to months depending on geographic scale), and the range of flows that could be assessed with repeatable measures was limited to flows less than approximately 56.6 m^3/s due to safety and duration.

Efforts to develop more robust habitat assessments using 2-D modeling platforms over a large range of flows were re-initiated in 2010. Technology used for remote sensing and direct measurements had improved and become widely available. Different iterations of WUA and habitat mapping guilds could be applied to 2-D hydrodynamic model outputs. Modeling started as an effort to subsample the restoration reach (Alvarez et al. 2015(b)), but eventually data collection for the entire restoration reach was completed and a 64-km hydrodynamic model was developed for the 2011-2012 condition (Bradley 2015). Deficiencies in resolution of the terrain on which the model was run, however, limited its use. The most important deficiency was along the margins of the low flow channel, where the majority of juvenile rearing habitat occurs. Available technology for bathymetric surveys improved by 2016, and multibeam sonar was used to collect more detailed terrain upon which a second hydrodynamic model was developed for the restoration reach (Bradley 2018). That model has since been widely used within the TRRP and serves as the foundation for this habitat synthesis report.

Development of habitat capacity metric

With renewed interest in 2-D hydrodynamic models to predict habitat quality and quantity over a broad range of flows and spatial scales came the desire to improve upon existing HSC. The desired improvements centered around the fact that previous direct observation efforts were heavily weighted by locations where fish were present and that detection probability remained unaddressed. Improvements were targeted to benefit the Stream Salmonid Simulator (S3) fish production model (Perry et al. 2018a) that was in development. Improved HSC would aim to develop density-dependent sub models that apply to upper thresholds of fish density in differing physical habitat (Pinnix et al 2019).

A year-long effort investigated sampling techniques that would improve fish density predictions (Pinnix et al. 2016). Thereafter, a study was developed that leveraged existing 2-D hydrodynamic models (Alvarez et al. 2015(b)) to distribute sampling across the range of habitats that existed at a site during the specific period when sampling occurred (Pinnix et al. 2019). Areas of relatively homogenous habitat, which roughly reflected the size of the 2-D hydrodynamic modeling mesh elements, were selected from gradients along combinations of depth, velocity, and distance to escape cover and spatially distributed along the length of each 2-D model site (Pinnix et al. 2019). This sampling design was paired with a ‘dual-diver’ simultaneous observation approach that enabled accounting for detection probability. The study was conducted for two consecutive years, in 2013 and 2014, and 4,568 habitat units were surveyed.

Fortuitously, the first year of the study coincided with one of the largest spawning escapements for Chinook Salmon since extensive run-size estimation efforts began in 1978 (Gough et al. 2021; in draft). The large run provided a favorable data set to develop a metric for upper limits of fish density which could be used as an indicator of physical habitat quality. The use of a zero-inflated N-mixture model, inclusion of random effects, and quadratic and interaction terms for physical variables allowed for the development of a new habitat quality metric which accounted for detectability, the patchy distribution expected from an emerging and migrating population, and the interactions of physical characteristics over the ranges in which they occurred (Pinnix et al. 2019, Som et al. 2018). The model arising out of this analysis allows for the direct computation of an upper limit for the number of fish per area, defined as the upper 95th percentile in juvenile fish density, which is referred to as capacity hereafter, and interested readers are encouraged to consult Perry et al. (2018b) for a more detailed description of the theoretical and computational steps for generating capacity estimates.

This report represents the first reporting of capacity results over the entire geographic extent of the 2016 hydrodynamic model developed by the TRRP (Bradley 2018). However, capacity has previously been used in the design process (Yurok Tribe 2021) and in the evaluation of restoration site evolution (Gaeuman et al. 2021) to compare hypothetical and actual geomorphic change over comparatively small areas. Capacity has also been used to inform sub-models of the S3 fish production model (Perry et al. 2018a) and was officially adopted by the TRRP Fish workgroup in 2020 as the preferred measure of physical habitat (Lindke 2020). While spatially expansive, analysis in this report is limited temporally to 2016 channel conditions and is intended to be revisited when a subsequent 64-km hydrodynamic model is developed for river conditions in the future.

Purpose

The TRFE identified rearing habitat for juvenile life stages as a limiting factor determining Trinity River salmonid production. Thus, one of the main goals of the TRRP is to improve rearing conditions through channel rehabilitation alongside flow and gravel augmentation (USDI 2000). This report specifically assessed habitat in what TRRP identified as the 64-km restoration reach of the mainstem Trinity River most impacted by TRD management, beginning at Lewiston Dam and ending just above the North Fork Trinity River confluence. Terrain and hydraulic data developed from aerial and ground-based surveys in 2016 were utilized by Bradley (2018) for hydrodynamic modeling. The capacity model from Som et al. (2018) provided number of fish estimates from which the 95th percentile values of fish density were observed and associated with variables of depth, velocity, and distance to wetted cover. The hydrodynamic model from Bradley (2018) provided spatial outputs of depth and velocity throughout the restoration from which spatial outputs of capacity were estimated at a range of 24 flows (4.2 – 623.0 m^3/s) for fry (<50 mm) and presmolt (>50 mm) life stages. The purpose of this synthesis report was to utilize juvenile Chinook Salmon estimates from the spatially explicit, flow specific habitat capacity model specific to the Trinity River restoration reach as a primary metric to assess TRRP rehabilitation effectiveness with the following four objectives:

Objective 1: Evaluate rearing habitat capacity for areas that have received mechanical rehabilitation and those that have not.

Objective 2: Evaluate rearing habitat capacity between rehabilitation sites.

Objective 3: Evaluate topographic attributes that contribute to habitat capacity.

Objective 4: Evaluate the availability of habitat capacity within reaches given frequency and duration of flows during the critical rearing period.

Methods

In summary, we utilized outputs from a Chinook Salmon juvenile capacity model (Som et al. 2018) in ArcGIS, Excel, and program R (R Core Team 2020) and evaluated juvenile Chinook Salmon capacity estimates standardized as capacity of fish per linear meter (C), the relationship of C to flow (Q) specified at different spatial scales, physical variables as drivers of C, and the relationship of C to changes in flow duration. Chinook Salmon rear in the Trinity River restoration reach in the winter and emigrate through the end of May in most years. The months of January through May were considered the critical rearing period for this report in order to capture the primary phenology of fry and presmolt life stages. Flow duration analysis was used to determine a frequent range of flows during the critical rearing period, and juvenile capacity (C) was related to that range of flows. We first assessed fry and presmolt C in relation to Q throughout seven hydrologically distinct sub-reaches identified as Maximum Fisheries Flow (MFF) reaches (DWR 2007). We compared C to Q relationships in rehabilitated and non-rehabilitated areas within those sub-reaches, where rehabilitated areas included any rehabilitation sites within a given sub-reach and non-rehabilitated areas included all areas outside of those sites within a given sub-reach. The C to Q relationship at 24 rehabilitation sites constructed in 2016 or earlier was compared using an integrated area under the curve metric (I), and minimum C values (C_{min}) were evaluated as indicators of habitat limitation to fish capacity. Functions of C were evaluated at the site-scale with distance from dam and rehabilitation construction year, and at the reach-scale with physical channel metrics including active channel width and topographic relief. Changes in flow duration from accretionary flows and scenarios of increased baseflow management were evaluated for their effect on C at the MFF reach and restoration reach scale.

Detailed analysis through which this report's four objectives were accomplished are described alongside their results in following sections, where we convey our application of the capacity model as a tool that has developed sequentially for physical habitat assessment regarding hydraulics and wetted cover conditions. In Objectives 1 and 2, we evaluate hydraulics and distribution of cover over a range of flows; in Objective 3, we assess hydraulics and cover conditions in different aspects of channel form that affect hydraulics; and in Objective 4, we attempt to assess habitat availability with respect to changes in hydrology. We emphasize that while hydrology was used to inform the flow range over which we considered capacity in the first three objectives, it was not an assessment of habitat availability but of channel form.

Analysis and Results

Objective 1: Evaluate Chinook Salmon rearing habitat capacity for areas that have received mechanical rehabilitation and those that have not

Output from the capacity model spanned 24 discharges ranging from 4.2 to 623.0 m^3/s. A first step in this analysis was to determine the range of flows relevant for assessing juvenile salmonid habitat. The MFF reaches (DWR 2007) represent sub-reaches of the Trinity River restoration reach relevant to habitat capacity assessments in this report (Figure 1). While some reaches have undergone more rehabilitation with differing design approaches than others, the hydrologic distinction of the MFF reaches was appropriate in our evaluations of capacity to different flows and hydraulic conditions.

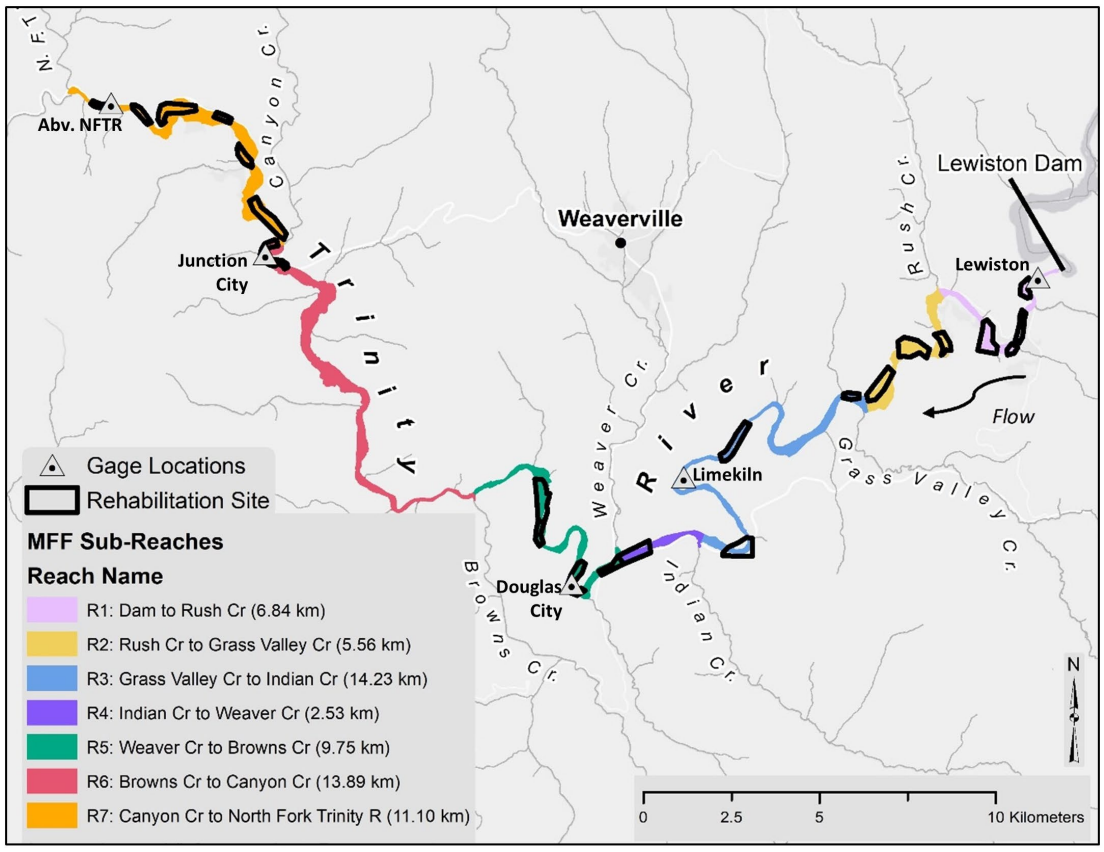

Figure 1. Trinity River restoration reach from Lewiston Dam to the North Fork Trinity River confluence divided into seven MFF reaches (specified by tributary confluence and length in legend). A total of 24 rehabilitation sites (outlined in black) and five USGS gaging locations (dotted triangles) were used in this study's assessments.

For each MFF reach, we developed flow duration curves for the critical juvenile rearing period, defined as January 1 through May 31 using mean daily flows from USGS Trinity River gages located at Lewiston, Limekiln Gulch, Douglas City, Junction City, and above the confluence of the North Fork Trinity River, as well as tributary gages at Rush Creek and Indian Creek (Figure 2, Table 1). We found flows (Q) during critical rearing months are less than 99.1 m^3/s from 82 – 90% of the time throughout the restoration reach (Table 2). Therefore, flows up to 99.1 m^3/s constituted the vast majority of juvenile rearing conditions and served the purposes of Objective 1 (Table 2). The flows over which we analyzed rearing habitat capacity therefore include 14 of the 24 capacity estimated discharges modeled by Bradley (2016) and Som et al. (2018) as follows: 4.2, 8.5, 10.6, 12.7, 17.0, 21.2, 25.5, 29.7, 35.4, 42.5, 56.6, 70.8, 85.9, and 99.1 m^3/s.

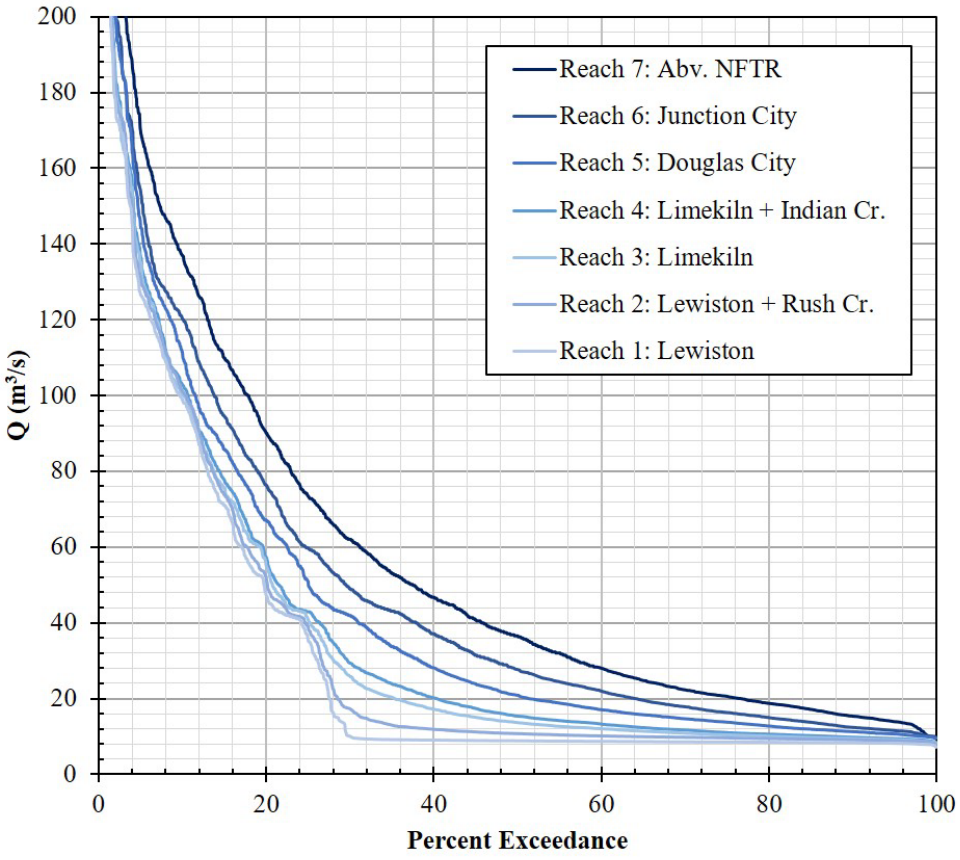

Figure 2. Daily flow duration curves from seven gaging stations on the Trinity River restoration reach. Curves are graduated with darker shades as distance downstream increases. Daily average flows during months January through May were evaluated over the period of record (POR) from WY2005 – 2020. Data from 'Abv. NFTR' was incomplete in WY2005 and was limited to period of record from WY2006 – 2020.

Table 1. Flow duration summary statistics for each MFF reach and its respective USGS stream gage locations.

Exceedance Probability	Q (cms)						
	Reach 1: Lewiston	Reach 2: Lewiston + Rush Cr.	Reach 3: Limekiln	Reach 4: Limekiln + Indian Cr.	Reach 5: Douglas City	Reach 6: Junction City	Reach 7: Abv. NFTR
10%	98.5	101.0	101.6	102.8	110.7	120.1	137.1
20%	47.3	51.7	54.9	57.2	67.1	76.2	90.0
30%	9.5	17.3	25.9	29.3	41.9	49.0	62.0
40%	9.0	11.8	17.2	20.2	28.1	37.1	46.7
50%	8.8	10.7	13.6	15.3	20.8	27.6	36.5
60%	8.7	10.1	12.0	13.2	17.0	21.9	28.0
70%	8.6	9.8	10.9	11.7	14.6	17.8	22.3
80%	8.4	9.4	10.1	10.6	12.7	15.0	18.7
90%	8.3	9.1	9.4	9.8	11.2	12.4	15.3

Table 2. Exceedance probability of 99.1 m3/s calculated from flow duration curves from seven USGS gaging stations.

MFF Reach	USGS Gage Name, ID	Period of Record for Jan 1 - May 31	Exceedance Probability at 99.1 m^3/s
Reach 1 (R1)	Lewiston, 11525500	2005 – 2020	9%
Reach 2 (R2)	Lewiston, 11525500 + Rush Cr, 11525530	2005 - 2020	10%
Reach 3 (R3)	Limekiln, 11525655	2005 – 2020	10%
Reach 4 (R4)	Limekiln, 11525655 + Indian Cr, 11525670	2005 – 2020	10%
Reach 5 (R5)	Douglas City, 11525854	2005 – 2020	12%
Reach 6 (R6)	Junction City, 11526250	2005 – 2020	14%
Reach 7 (R7)	Abv North Fork Trinity R., 11526400	2006 – 2020*	18%

**Data incomplete for WY2005.*

Daily exceedance of 99.1 m^3/s during the juvenile Chinook Salmon rearing period differs less than 10% within the restoration reach, making a good upper end of the flow range for habitat evaluations. However, it is worth noting the differences in exceedance percentiles at other flows can be much greater. This is highlighted by the 50% daily exceedance which is 8.5 m^3/s at Lewiston, 20.8 m^3/s at Douglas City, and 35.9 m^3/s at the downstream most end of the restoration reach. That is, the 50% exceedance daily flows at the downstream end of the restoration reach are four times the upstream end, and on average 2.6 times greater at the

downstream end. These flow duration discrepancies during the critical rearing period within the restoration reach are further evaluated later in this report.

Chinook Salmon fry and presmolt capacity estimates were summed over each MFF reach for each of the 14 modeled flow rates from 4.2 - 99.1 m^3/s. In ArcMap, the spatial output for capacity comes in a shapefile for each associated flow rate, where each shapefile is made up of a large number of mesh elements with an extent expansive enough to cover areas inundated at very high flows (up to 566.3 cms). Each mesh element provides an area, given its physical conditions, in which number of fish is estimated in the spatial output; there are no instances of capacity less than zero. There are many instances where there is no fish capacity within mesh elements, which changes at various flow rates. To reduce file size and processing time, each spatial capacity output specific to a given flow rate was selected by attribute where capacity was greater than zero and exported to a new shapefile. We used spatial and attribute joining and an 'Integrate Field over Polygons' tool in ArcMap to batch process summed capacities over areas. Capacity sums for each MFF reach and flow were divided by the reach length to yield capacity per meter stream length (fish/m) herein expressed as *C* (Figure 3).

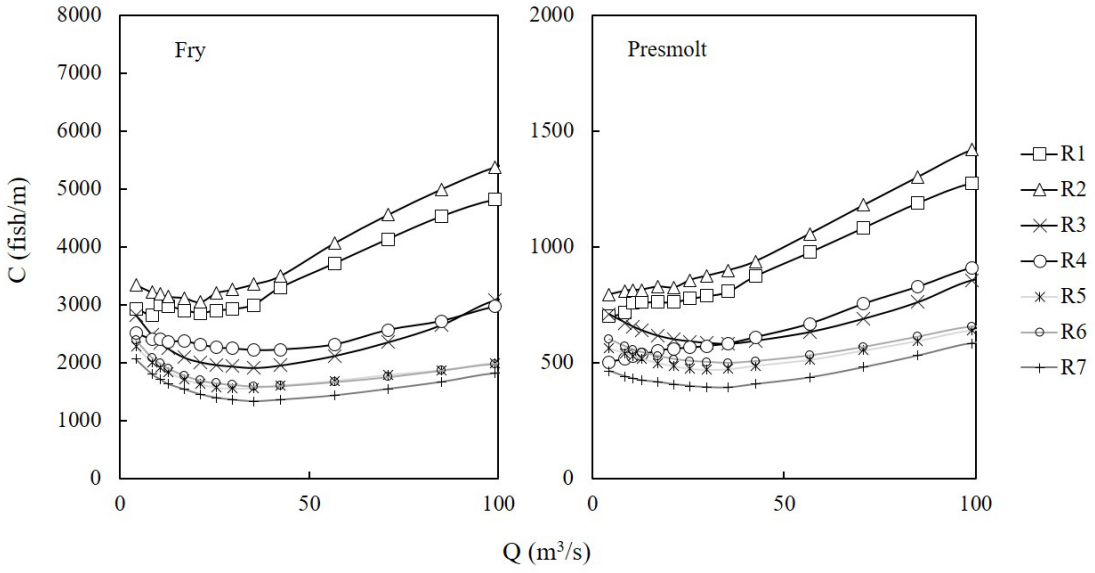

Figure 3. Chinook Salmon fry (left panel) and presmolt (right panel) C estimated at 14 flows from 4.2 – 99.1 m3/s among seven MFF reaches. Some curves overlap (e.g. areas of R3 and R4; R5 and R6).

Throughout most MFF reaches, fry *C* started relatively high at the lowest flow (4.2 m^3/s) and had a negative response to flow until about 21.2 – 35.4 m^3/s, at which point the capacity-flow relationship became positive to varying degrees. Presmolt *C* responded with a similar 'habitat dip' in response to mid-range flows in some but not all cases. MFF reaches with a mostly positive response to *Q* include R1, R2, and R4 for presmolt *C*. The shape of the curve for fry and presmolt *C* to flow was generally similar among sub-reaches, with the main differences being the broadness of the habitat dip over flows and the magnitude of *C*. Fry and Presmolt *C* was greatest over all flows for both fry and presmolt in R2, followed by R1. Reaches R3 and R4

had similar ranges of fry and presmolt *C*, as did reaches R5 and R6, followed by the lowest ranges of fry and presmolt *C* in R7. A negative trend between capacity magnitude and distance from dam became apparent throughout the MFF reaches.

Adopting methods from previous Trinity River habitat assessments and in an effort to compare capacity between different areas, we summarized capacity into a single number over multiple flows in a given area. Specifically, we quantified the overall capacity for both life stages across 4.2 – 99.1 m^3/s by integrating the areas under the *C* to *Q* curves (*I*) according to:

$$I = \int_{4.2}^{99.1} CQ\, dQ \qquad (1)$$

This computation was preformed numerically using the MESS package 'auc' function in statistical program R (R Core Team 2020). Resulting *I* values are large dimensionless values, so *I* values were normalized (I_N) to a scale from 0 to 1 by dividing *I* with the greatest *I* value (I_{max}) among all reaches:

$$I_N = I / I_{max} \qquad (2)$$

MFF reaches were summarized by proportion length rehabilitated, number of rehabilitation sites, and normalized fry and presmolt capacity (Table 3). MFF reaches R2, R1, R5, and R7 have at least 44% of their length rehabilitated, while R6 has the least (10%) length rehabilitated. Overall, about one third of the 64-km restoration reach has been rehabilitated with 24 rehabilitation sites completed up to year 2016. Despite having one of the greatest proportions rehabilitated and number of sites, R7 had the least capacity.

Table 3. MFF reaches in the Trinity River and their respective number of rehabilitation sites, proportion length rehabilitated, and normalized integrated area under the capacity-flow curve (I_N) among reaches.

MFF Reach	No. Rehabilitation Sites	Length (km) Rehabiliated	Total Length (km)	% Length Rehabilitated	Fry I_N	Presmolt I_N
R1	5	3.27	6.84	48%	0.84	0.86
R2	3	3.27	5.56	59%	1.00	1.00
R3	3	2.84	14.23	20%	0.58	0.62
R4	1	0.90	2.53	36%	0.58	0.62
R5	4	4.25	9.75	44%	0.39	0.46
R6	2	1.40	13.89	10%	0.40	0.48
R7	6	5.32	11.10	48%	0.36	0.42
Total	*24*	*21.26*	*63.90*	*33%*	-	-

We then evaluated differences in Chinook Salmon juvenile capacity between rehabilitated and non-rehabilitated areas of MFF reaches (Figure 4). Non-rehabilitated areas

included any part of a reach outside of a rehabilitation area, and proportions of rehabilitated areas are described in Table 3. While some reaches have a greater proportion of rehabilitation sites than others, the normalized *C* metric allowed us to compare the *C* to flow (*Q*) relationship between reaches in rehabilitated versus non-rehabilitated areas.

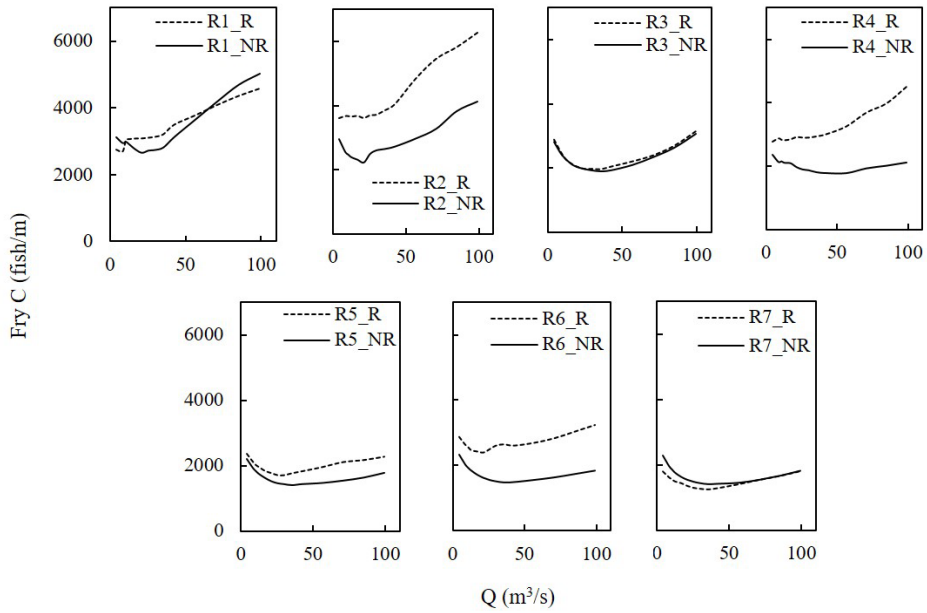

Figure 4. C to Q relationships in rehabilitated areas (dotted line) and non-rehabilitated areas (solid line) for fry Chinook Salmon in seven MFF reaches in the Trinity River. Some curves overlap with similar values (e.g. R3_R and R3_NR).

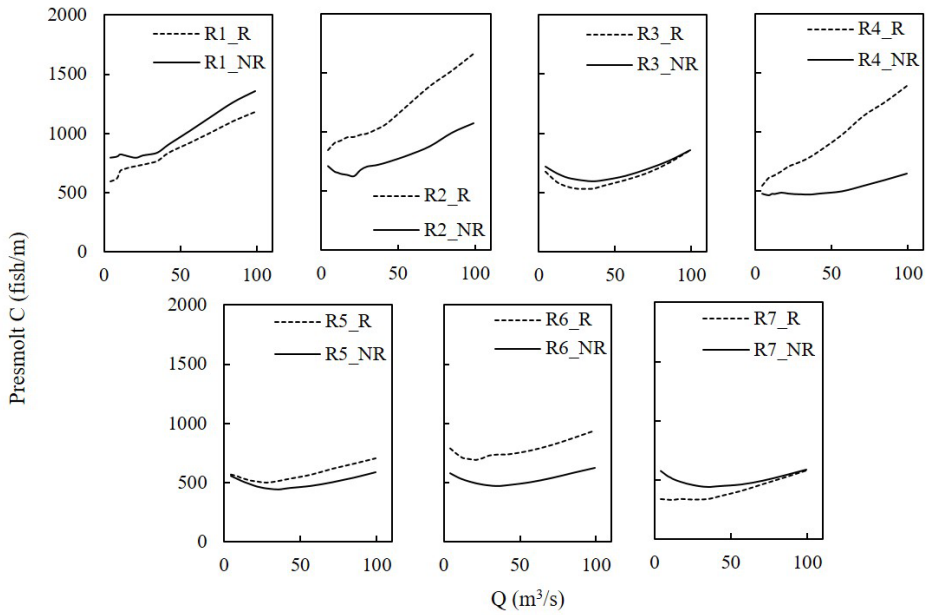

Figure 5. C to Q relationships in rehabilitated areas (dotted line) and non-rehabilitated areas (solid line) for fry presmolt Chinook Salmon in seven MFF reaches in the Trinity River.

In addition to generally decreasing capacities with increasing distance from dam, mean *C* was greater in rehabilitated areas than in non-rehabilitated areas among MFF reaches 2, 4, 5, and 6. Capacity in rehabilitated areas of MFF reach 2 exceeded any other area throughout the entire restoration reach. The difference in magnitude of capacity between non-rehabilitated and rehabilitated areas was similar in MFF reaches 2, 4, and 6. *C* of rehabilitated areas is marginally greater in reach 5. Notably, capacity in rehabilitated areas of reaches 1, 3, and 7 was about the same or less than in non-rehabilitated areas.

Objective 2: Evaluate Chinook Salmon rearing habitat capacity at rehabilitation sites

Capacity to flow relationship: the 'habitat dip'

We calculated Chinook Salmon capacities per unit length for fry and presmolt within the bounds of 24 rehabilitation sites constructed in 2016 or earlier, whose names and abbreviations are described in Table 4. We summarized the overall capacity for both life stages across that range of flows by integrating the areas under the *C* to discharge (*Q*) curves (*I*) described previously (Equation 1). To compare between sites, *I* values were then divided by the greatest *I* value (I_{max}) among all sites to produce normalized values (I_N) in a scale from 0 to 1 described previously (Equation 2).

Table 4. TRRP rehabilitation site names, their abbreviations, and their respective MFF reach names, distances from dam, and construction years.

MFF Reach	Rehab Site Name	Rehab Site Abbr.	KM from Dam	Construction Year
R1	Sven Olbertson	SVO	1.5	2008
R1	Deadwood	DW	2.5	2008
R1	Cableway	CBW	3.1	2008
R1	Hoadley Gulch	HG	3.6	2008
R1	Sawmill	SWM	5.1	2009
R2	Upper Dark Gulch	UDG	8.6	2008
R2	Bucktail	BT	10.7	2016
R2	Lowden Ranch	LDR	12.3	2010
R3	Trinity House Gulch	THG	13	2010
R3	Limekiln Gulch	LKG	19.9	2015
R3	Vitzum	VITZ	25.8	2007
R4	Lower Indian Creek	LIND	29.1	2015
R5	Upper Douglas City	UDC	29.8	2015
R5	Reading Creek	RC	32	2010
R5	Lower Steiner Flat	LSF	35.3	2012
R5	Lorenz Gulch	LZG	36.7	2013
R6	Upper Junction City	UJC	52	2013
R6	Lower Junction City	LJC	52.8	2013
R7	Hocker Flat	HF	54.4	2005
R7	Conner Creek	CC	56.5	2006
R7	Wheel Gulch	WG	58.1	2011
R7	Valdor Gulch	VLD	60.1	2006
R7	Elkhorn	ELK	61.8	2006
R7	Pear Tree	PTR	63	2006

We compared I_N for each life stage between sites (Figure 6). Upper Dark Gulch, Bucktail, and Lowden Ranch had the greatest capacity for both fry and presmolt life stages, which make up all rehabilitated areas in MFF reach 2. Sites with the least capacity for both fry and presmolts included Conner Creek, Hocker Flat, Elkhorn, and Valdor Gulch, all of which contribute to rehabilitated areas of reach 7. There is a general decline in rearing capacity with increasing

distance from the dam among sites, with exception to sites in MFF reaches 6 and 4. The range of relative I_N for fry is greater than that for presmolt.

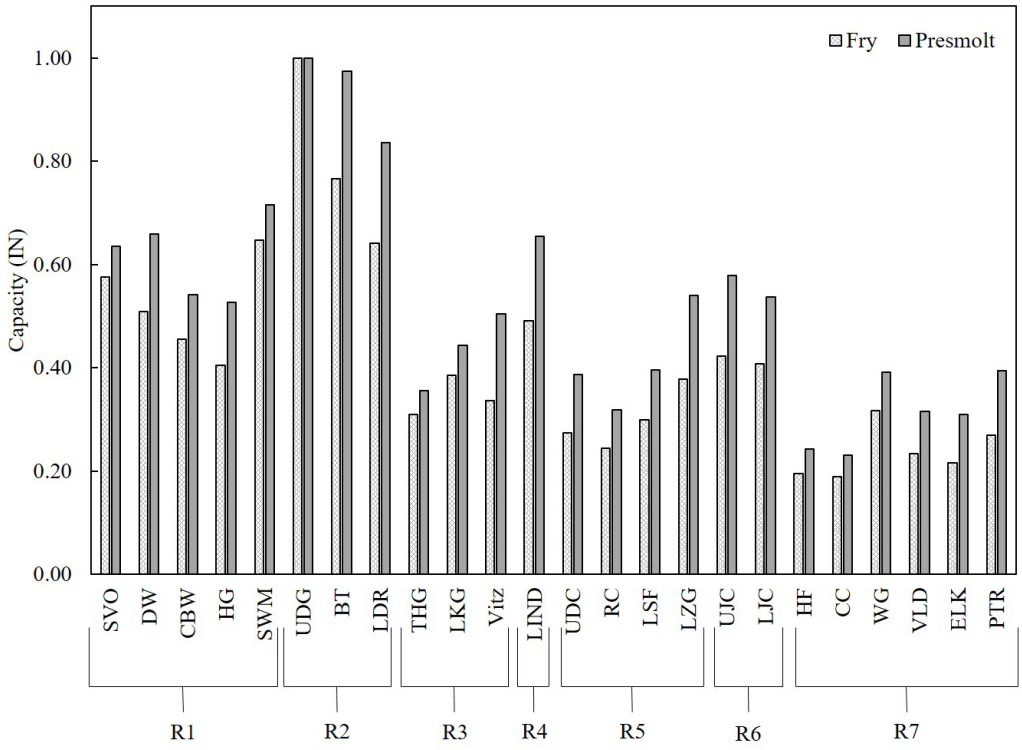

Figure 6. Integrated area (I_N) under the capacity-flow curve for fry (lighter shade) and presmolt (darker shade) at 24 rehabilitation sites. The I_N values are relative to the site with the greatest I value. Sites are labeled with their respective MFF reach and listed left to right in order from upstream to downstream.

The capacity response to flow within sub-reaches and restoration sites illustrates the 'habitat dip' from 8.5 m^3/s up until about 35.4 m^3/s or more. Similar habitat dips were observed in other studies that measured habitat with hydraulic variables in the restoration reach (USFWS and HVT 1999, Boyce et al. 2020). Within that limited habitat, slow water, access to cover, and hydraulic variability are presumably limited. For example, deep and fast flow conditions associated with the habitat dip may be occurring in a highly confined or incised channel with little lateral connectivity to instream vegetative cover, feathered edges, floodplains, and side channels. Because habitat rehabilitation aims to improve rearing conditions so that the habitat dip is minimized, we evaluated at what flows habitat minimums occur within rehabilitated sites.

In the habitat dip, minimum C (C_{min}) at most sites occurs over mid-range flows. Over all sites, C_{min} occurred from 8.5 to 56.6 m^3/s; the average flow associated with C_{min} is 26.0 m^3/s (SD 12.4 m^3/s). We found a moderate trend ($R^2 = 0.37$) where flows associated with C_{min} increased with distance downstream. Where site-scale C_{min} flows deviate from reach-scale C_{min} flows suggests rehabilitation efforts have mitigated the geomorphic conditions that result in the habitat dip. This was first illustrated in Objective 1 of this report when rehabilitated versus non-rehabilitated areas within MFF reaches were compared with their C to Q curves. A more in-depth

evaluation of this effect was illustrated by comparing individual site *C* to *Q* curves with non-rehabilitated *C* to *Q* curves within each MFF reach (Figure 7). Reaches 1 and 7 are represented in 2 graphs because the higher number of sites constructed in those reaches resulted in overlapping data that was difficult to read in one graph. Rehabilitation site presmolt curves (not plotted) display similar patterns and presmolt I_N is highly correlated to fry I_N (Pearson's $r = 0.94$).

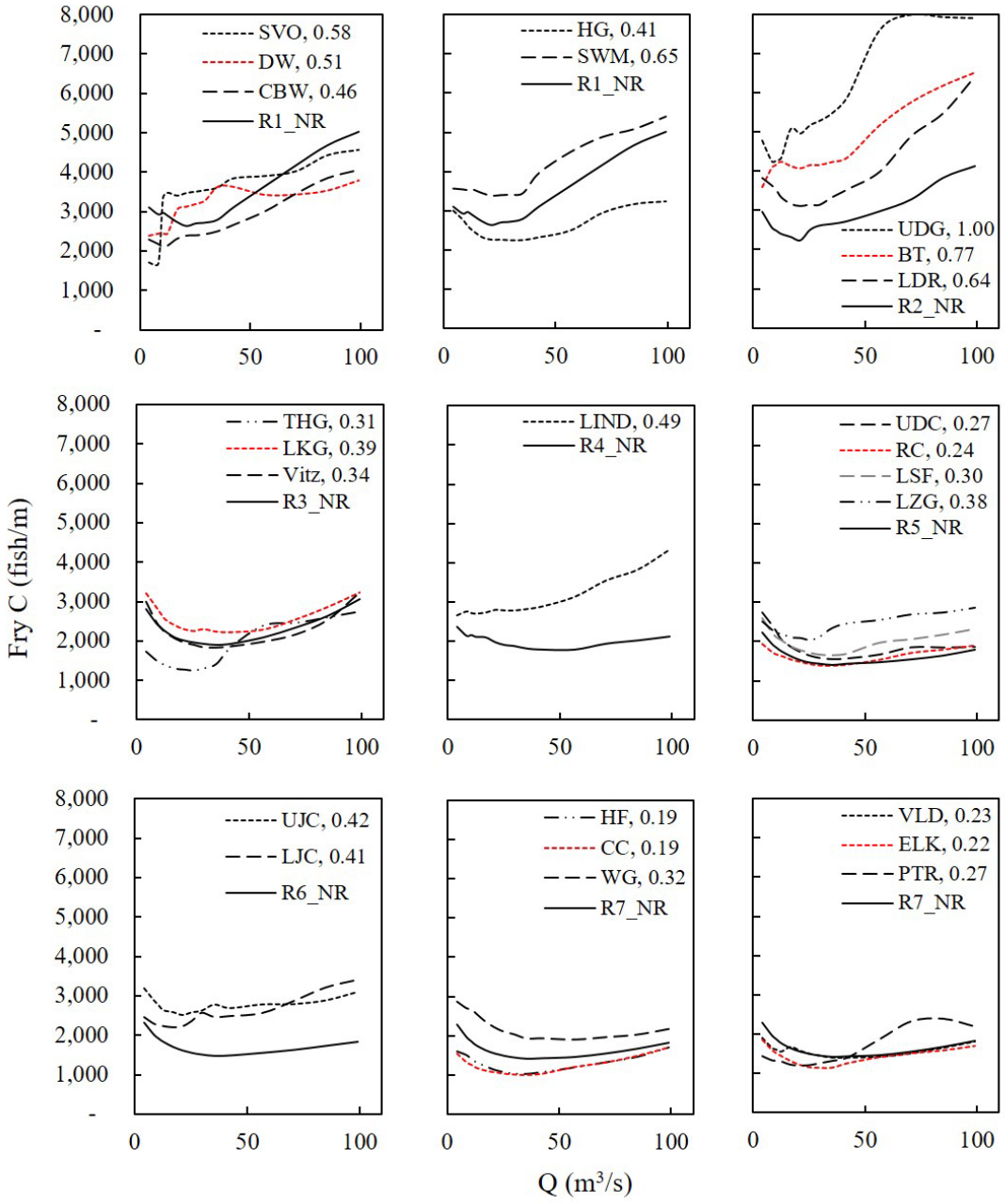

Figure 7. Rehabilitation site C to Q curves plotted with non-rehabilitated (NR) curves in seven MFF reaches that make up the Trinity River restoration reach. Sites are listed as they occur in distance from dam and an integrated area under the curve metric (IN) normalized among all sites is noted next to each site abbreviation. Some curves overlap with similar values (e.g. Vitz and R3_NR; UDC, RC, LSF, LZG, and R5_NR, etc.).

Comparing site-scale *C* to *Q* curves to their respective MFF reach *C* to *Q* curves in non-rehabilitated areas shows how rehabilitation efforts have improved fish capacity. Sites in R2 all have the greatest improved capacity from non-rehabilitated areas compared to other MFF reaches. Some reaches have rehabilitation sites that have either improved or reduced relative capacity compared to non-rehabilitated areas. For example, Wheel Gulch in R7 has much greater *C* than any other sites in R7 as well as any non-rehabilitated areas of R7. Conner Creek and Hocker Flat have reduced *C* compared to non-rehabilitated areas of R7, so techniques from those sites have not upheld and should likely be revised for future rehabilitation efforts in R7.

Capacity to flow relationship: potential spatial and temporal patterns

Trends in capacity among sites were evaluated by year of construction and distance from dam with linear models (Figure 8). Construction year was considered because design approaches and levels of effort have changed through time from simplistic berm and vegetation removal to implementing more complex instream features, realignments, off-channel habitat, and most recently with added emphasis on lowered floodplains and ponds at the valley scale. We found a moderate negative relationship (R^2 = 0.44 fry, 0.40 presmolt) between I_N and distance from dam, but as also seen in habitat assessments by Boyce et al. (2018), we detected no relationship between construction year and I_N. The relationship where habitat decreases in areas farther downstream has been observed previously with hydraulic metrics of habitat (Beechie et al. 2012, Boyce et al. 2020).

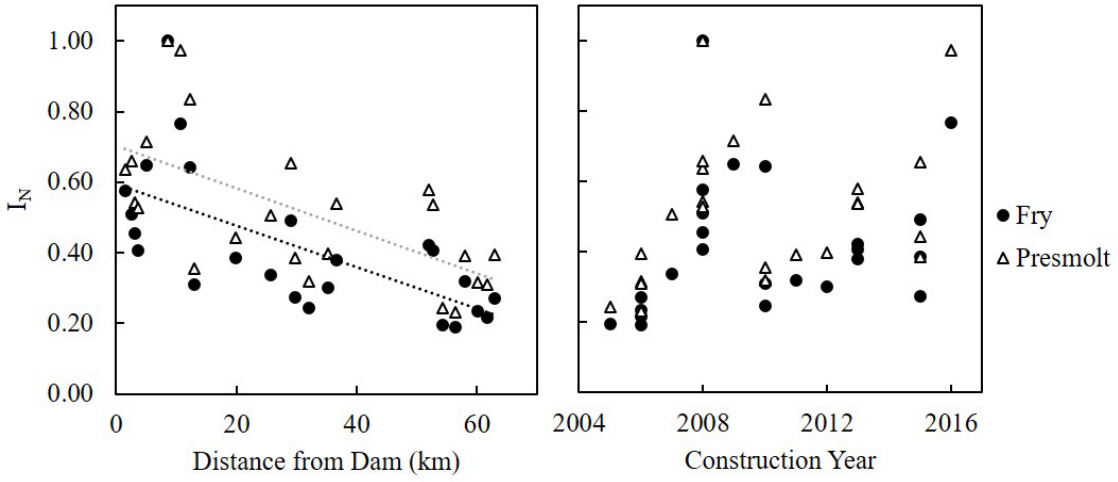

Figure 8. Potential variables related to juvenile IN were tested with linear models. Distance from dam (left) had a moderate negative relationship with fry and presmolt IN (R2 = 0.44, 0.40, respectively). Rehabilitation site construction year (right) had no relationship with fry or presmolt IN (R2 = 0.05, 0.10, respectively).

We selected a subsample of rehabilitation sites across the range of I_N values to visually compare spatial changes in capacity over a range of flows. We also selected sites that included a range of feature types such as single/multi-main channel, side channels, high-flow channels, feathered edges, and floodplains. These sites included Upper Dark Gulch (UDG, I_N = 1.00), Lowden Ranch (LDR, I_N = 0.64), Trinity House Gulch (THG, I_N = 0.31) and Hocker Flat (HF, I_N

= 0.19) (Figures 9 – 16). The figures display spatial differences in capacity with color ramps that grade from low to high capacity with yellow, orange, red, pink, and blue, with greatest capacities in blue. All figures are displayed with the same color ramp. Visualization at this scale reveals where specific features become inundated, connected, and how capacity responds to increases in flow and inundated area.

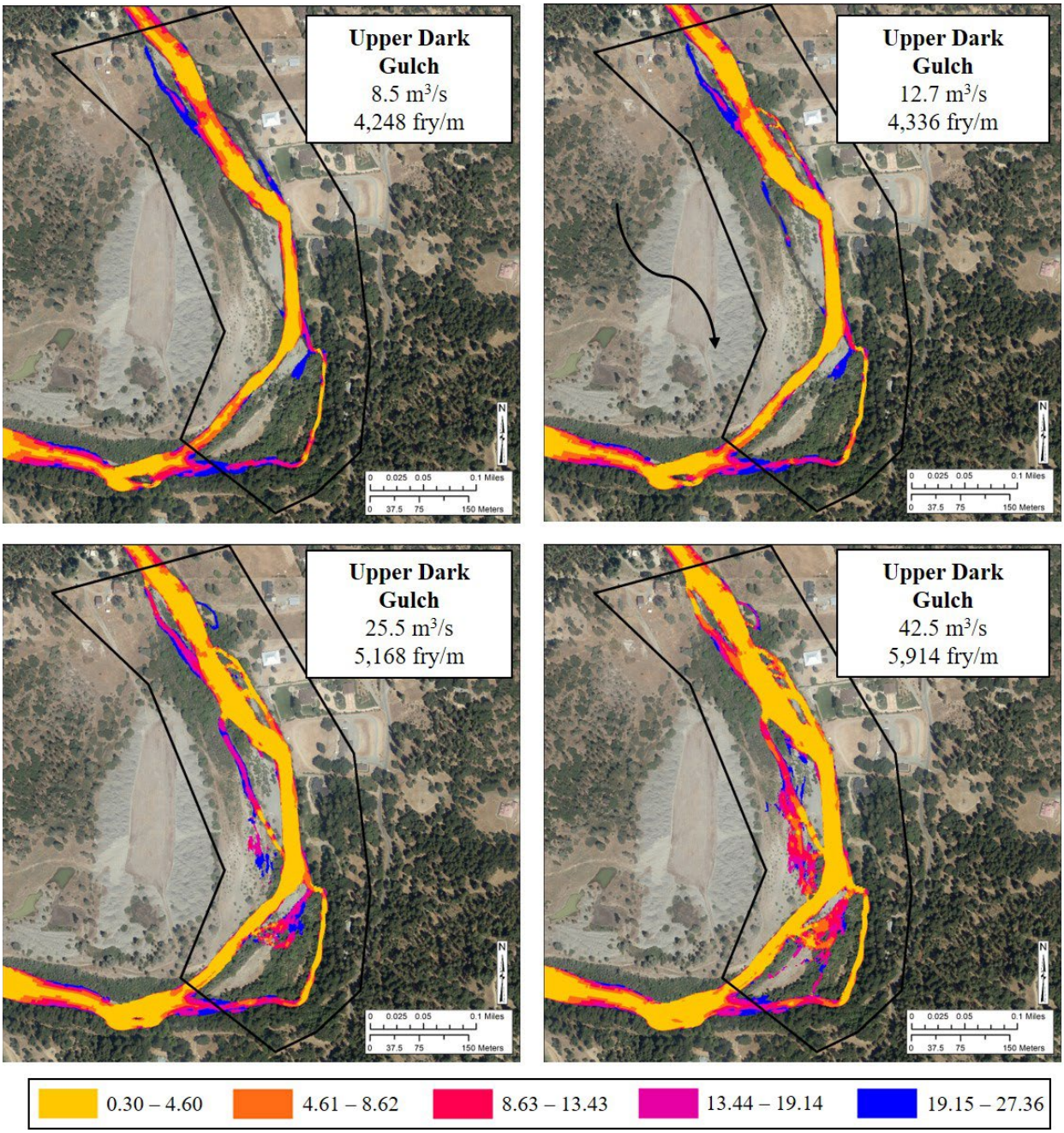

Figure 9. Heat maps of Upper Dark Gulch rehabilitation site (8.6 km from dam, 1.00IN) outlined in black display greatest fish capacities (pink, blue) in the upstream side-channel features. Capacities throughout the site increase from 8.5 to 42.5 m3/s, illustrating lack of a habitat dip. Arrow indicates direction of flow. Source: NAD83, US State Plane.

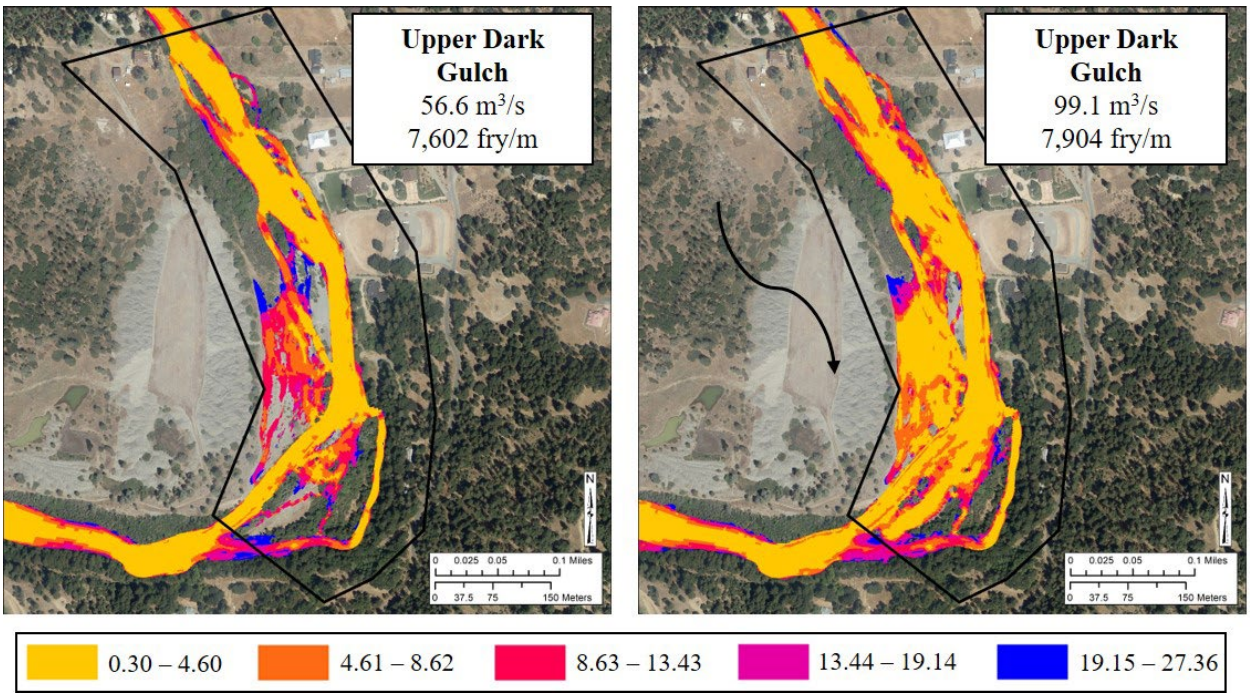

Figure 10. Heat maps of Upper Dark Gulch rehabilitation site (8.6 km from dam, 1.00 IN) display greatest fish densities (pink and blue) in the upstream side-channel features and increased capacity with floodplain inundation on river right. Capacities continue an increasing response to flows from 56.6 to 99.1 m3/s. Arrow indicates direction of flow. Source: NAD83, US State Plane.

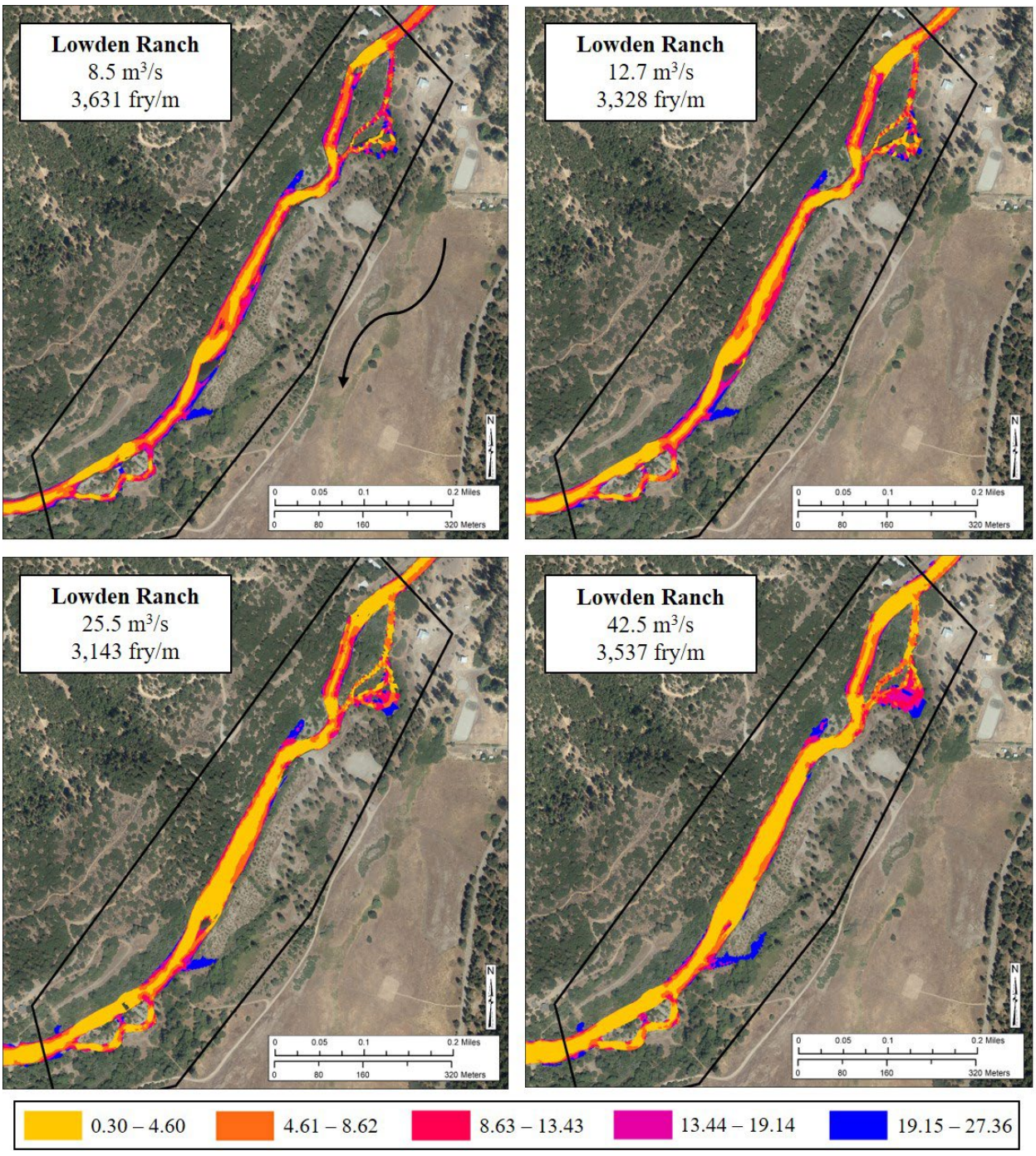

Figure 11. Heat maps of Lowden Ranch rehabilitation site (12.3 km from dam, 0.64 IN) display greatest fish capacities (pink and blue) in the upstream side-channel features. Capacities throughout the site are greatest at 8.5 m3/s and at 42.5 m3/s; they decline when inundated from 12.7 to 25.5 m3/s, illustrating the habitat dip. Arrow indicates direction of flow. Source: NAD83, US State Plane.

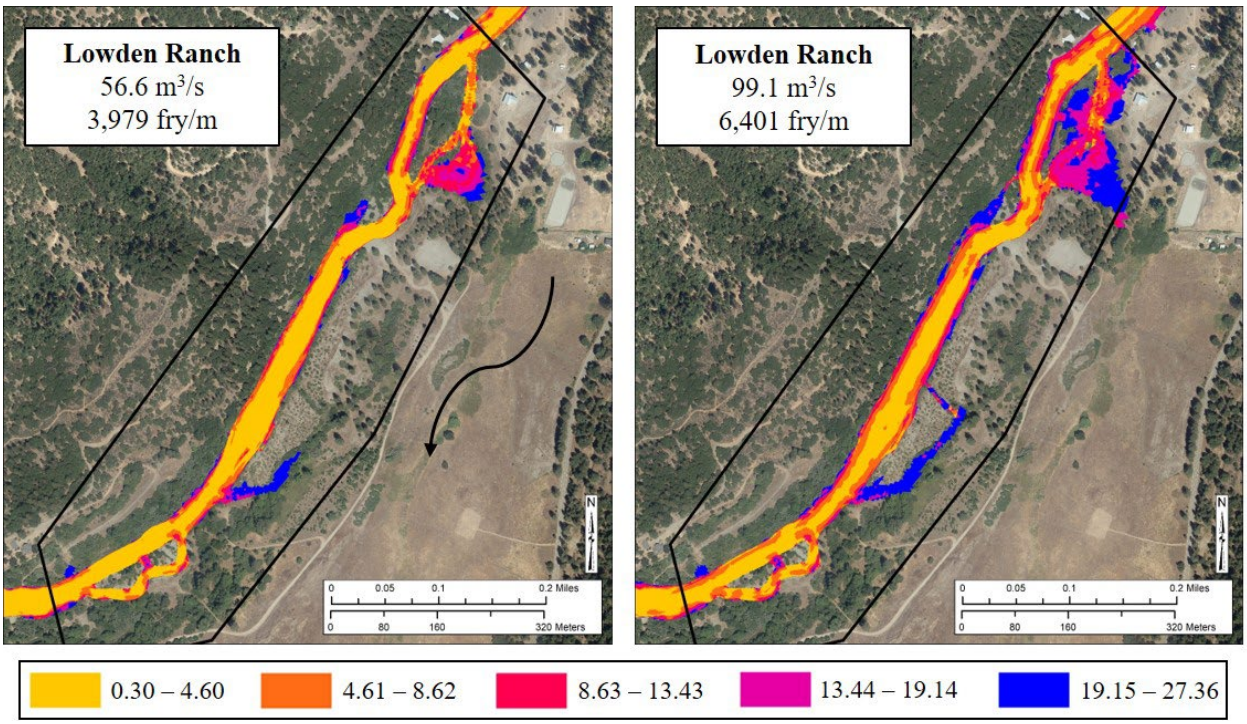

Figure 12. Heat maps showing how Lowden Ranch (12.3 km from dam, 0.64 IN) fish capacity increases with increasing flow rates from 56.5 to 99.1 m3/s due to greater areas of inundation in floodplain and side channel habitats with vegetative cover. Capacity is fry/m, with greater capacities in darker shades. Arrow indicates direction of flow. Source: NAD83, US State Plane.

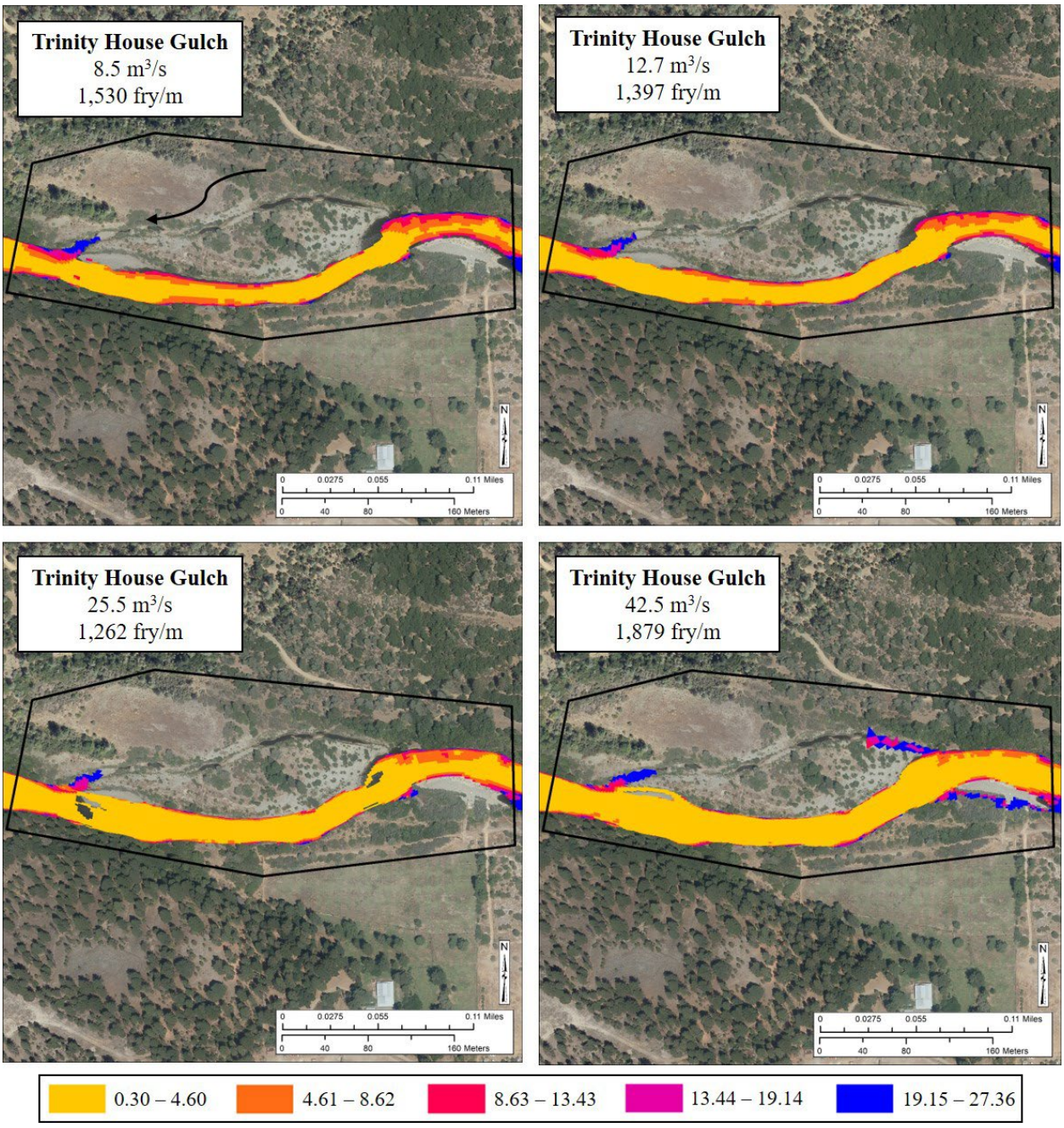

Figure 13. Heat maps of Trinity House Gulch rehabilitation site (13.0 km from dam, 0.31 IN) display greatest fish capacities (pink and blue) in the upstream side-channel features. Capacities throughout the site are greatest at 8.5 m3/s and at 42.5 m3/s; they decline when inundated from 12.7 to 25.5 m3/s, illustrating the habitat dip. Arrow indicates direction of flow. Source: NAD83, US State Plane.

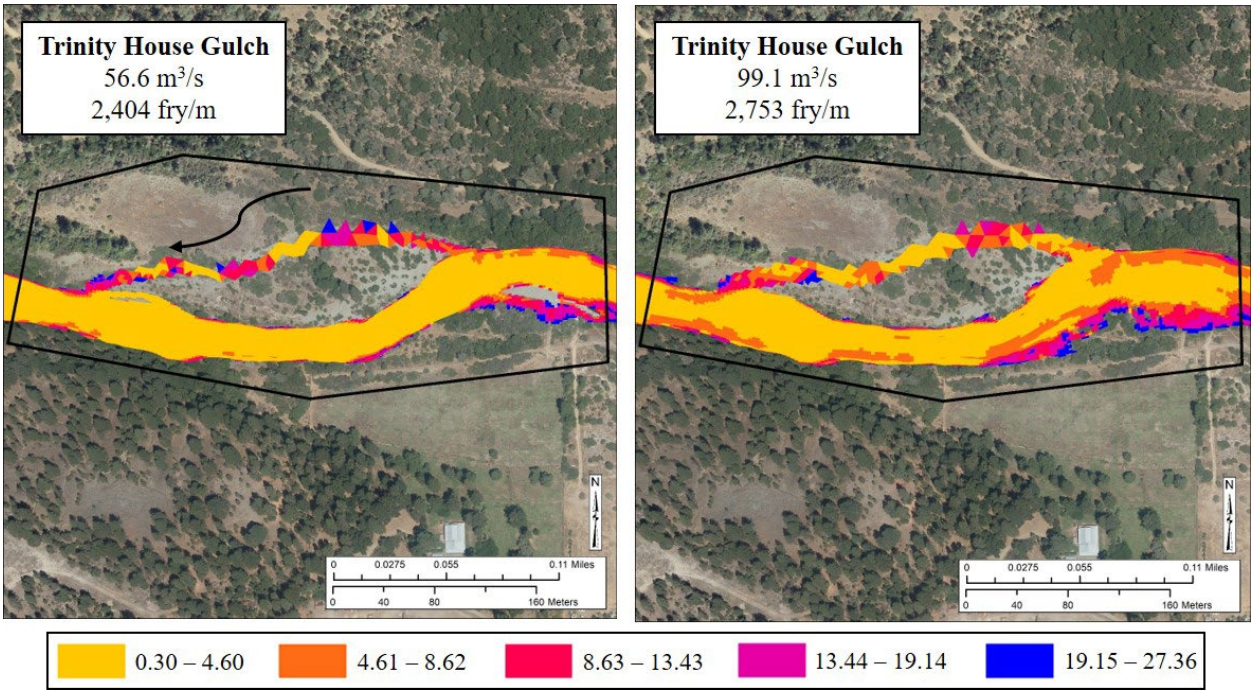

Figure 14. Heat maps of Trinity House Gulch rehabilitation site (13.0 km from dam, 0.31 IN) display greatest fish capacities (pink and blue) in the upstream side-channel features. Capacities throughout the site illustrate increasing capacity with flows from 56.6 to 99.1 m3/s with greater capacities in darker shades. Arrow indicates direction of flow. Source: NAD83, US State Plane.

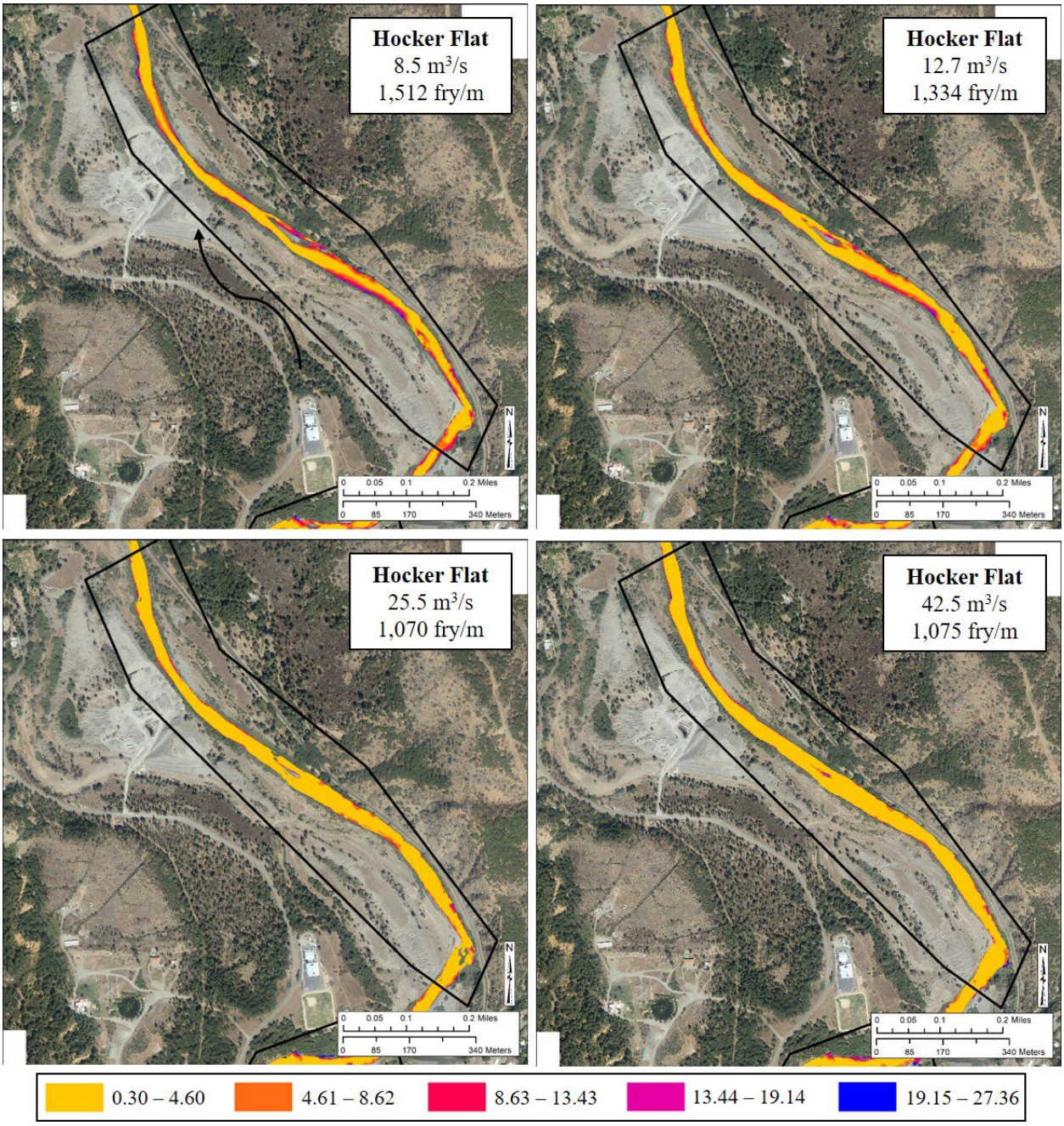

Figure 15. Heat maps of the Hocker Flat rehabilitation site (54.4 km from dam, 0.19 capacity-flow AUC) illustrating a declining trend in the capacity-flow relationship from 8.5 to 42.5 m3/s. Capacity is fry/m, with greater capacities in darker shades. There is little side channel or floodplain connectivity at these flows. Arrow indicates direction of flow. Source: NAD83, US State Plane.

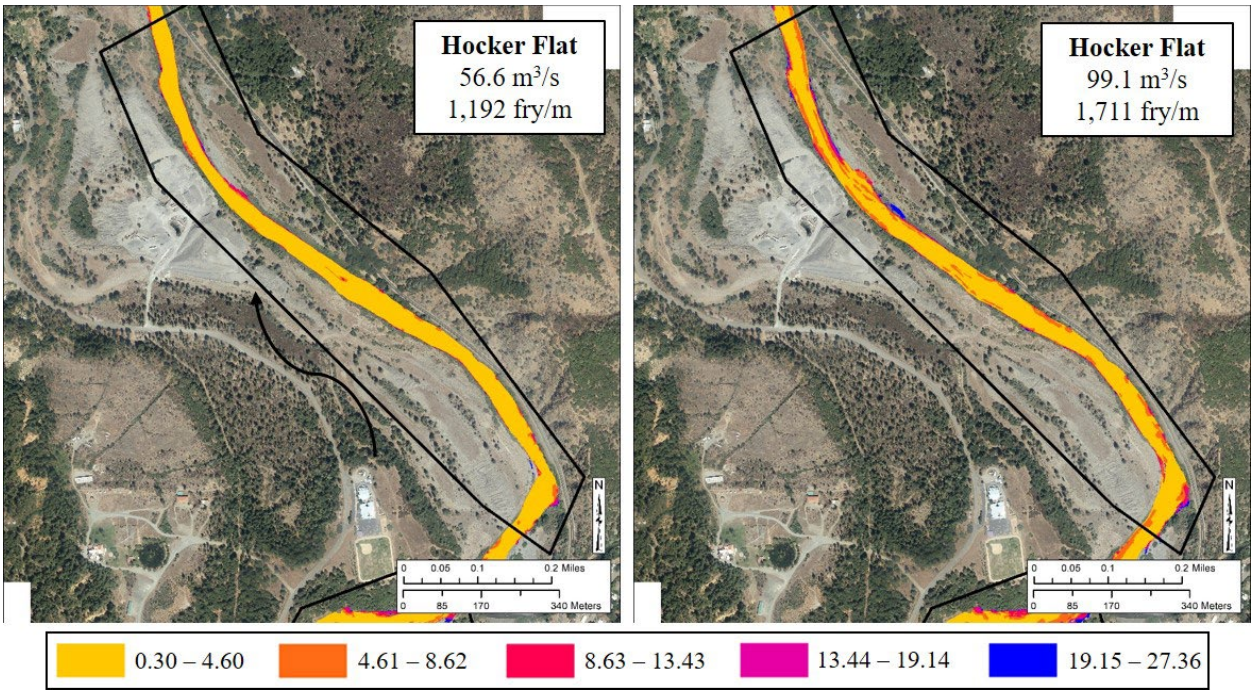

Figure 16. Heat maps of the Hocker Flat rehabilitation site (54.4 km from dam, 0.19 capacity-flow AUC) showing an increase in capacity with increasing flows from 56.6 to 99.1 m3/s. There appears to be inundated edges resulting in conditions with greater capacities (red and pink areas). Source: NAD83, US State Plane.

The spatial distribution of flow-specific capacities at rehabilitation sites reveal capacity 'hot-spots' mostly in side channel features with low velocities and where inundation in vegetated areas occurs. Figures 9 and 10 illustrate how capacity is greatly increased with floodplain inundation in the Upper Dark Gulch site. Capacity was limited when habitat was confined within the main channel up to mid-range flows at Trinity House Gulch (Figures 13 and 14) and over all flows at Hocker Flat (Figures 15 and 16). The habitat dip was spatially illustrated in Lowden Ranch, Trinity House Gulch, and Hocker Flat (Figures 11 – 16) where there generally was a declining trend in capacity with increasing flow rates that changed to an increasing trend around 42.5 m^3/s. The capacity-flow relationship at Upper Dark Gulch has very little habitat dip and was illustrated as capacity increased with increasingly inundated area (Figures 9 and 10). The maps reveal how capacities tend to decline in the main channel with increasing flows, emphasizing the importance of connectivity to side channel and floodplain habitats.

Outliers in the distance-from-dam relationship may call for further investigation of rehabilitation techniques and levels of effort. For example, Bucktail, Upper Dark Gulch, Sawmill, and Trinity House Gulch are all between 5.1 and 13.0 km from the dam, but Upper Dark Gulch, Bucktail, and Sawmill have much greater capacity (1.00, 0.77, and 0.65 I_N, respectively) than Trinity House Gulch (0.31 I_N). It appears that Trinity House Gulch has areas of high rearing capacity in its side channel only at higher flows while the majority of available habitat is within the main channel (see appendix). Upper Dark Gulch, Bucktail, and Sawmill all foster areas of greater capacity at lower flows and have greater areas of side channel features compared to Trinity House Gulch. Additionally, the varying hydrologic and geomorphic characteristics of reaches likely play a role in rehabilitation site effectiveness for juvenile

capacity. For example, Trinity House Gulch is in MFF reach 3 where there's a more confined canyon setting compared to other reaches upstream.

Objective 3: Evaluate topographic attributes that contribute to habitat capacity

Topographic attributes of the riverine landscape determine how flow interacts with the land to produce variable hydraulic environments over the range of discharges. In this section we evaluate two physical metrics and their relationship to physical habitat quality as measured by capacity. One metric quantifies topographic variability within the stream channel and the other involves how the inundated area available to the aquatic ecosystem changes with discharge.

Background and description of physical metrics

The hypothesis that complex channel morphology provides the basis for diverse, high-quality physical aquatic habitat is a core tenet of the TRRP rehabilitation strategy (TRRP and ESSA 2009). The precise meaning of "complex channel morphology," however, is unclear, and widely accepted metrics for quantifying it are lacking. Although a number of quantitative measures for assessing morphologic variability have been proposed in the literature, few have been applied to studies other than the ones in which they were introduced, and none are clearly linked to specific habitats attributes. Examples include the use of Moran's I by Madej (1999), who used that statistical method to track changing degrees of spatial autocorrelation of residual depth profiles (Lisle 1987) over time in a stream subject to periodic disturbances. Trainor and Church (2003) applied a dissimilarity index computed from the standardized differences in the mean values of physical variables in different stream reaches and showed that high dissimilarity values correspond to significant differences in key stream characteristics. Bartley and Rutherfurd (2005) presented several statistical measures developed from cross section shape, longitudinal channel profiles, or substrate grain size distributions that could differentiate between reaches of a stream that had or had not received large sediment inputs from upland gully erosion. Rayburg and Neave (2008) proposed a dozen measures of cross sectional and longitudinal geometry to characterize the asymmetry of a variety of bedforms and concluded that the measures are useful for highlighting the complexity of natural rivers.

Other authors have approached the question of how complexity relates to ecological function through the application of habitat classification systems (Bisson et al. 1982; Hawkins et al. 1993). With this approach, the aquatic environment is partitioned into a mosaic of habitat patches with differing ecological functions. Horan et al. (2000) provide an example of this approach by describing a "habitat complexity index" computed by combining the scores assigned to a set of physical variables, where the scores assigned to each variable depend on the expected relationship between the variable and fish density. As expected, the complexity indices so obtained correlated with observed fish densities. Yarnell et al. (2006) applied Shannon's Diversity Index, a statistic drawn from the field of landscape ecology, to evaluate the relative dominance of different types of aquatic habitat patches. They then compared the diversity scores to a measure of relative sediment supply and to the proportion of the streambed occupied by

structural elements like boulders and large wood. Although Yarnell et al. (2006) were successful in demonstrating an apparent link between higher habitat diversity and sediment supply rates of intermediate magnitude, neither they nor Horan et al. (2000) bridged the gap that separates habitat diversity and morphological complexity.

Technological advances in recent years have made new approaches for evaluating physical complexity possible. In particular, the availability of LiDAR, multibeam sonar, and Structure-from-Motion (SfM) photogrammetry makes the development of accurate, high-resolution terrain models accessible to many researchers and resource managers. Such terrain models make it possible to define new complexity metrics that incorporate 3-dimensional attributes of the landscape that correspond to habitat availability and quality far better than the simple 1- and 2-dimensional metrics proposed in past decades. Among the relative early attempt to define morphologic complexity in 3-dimensions are a set of metrics described in a report intended to advance new conceptual models for guiding TRRP activities (Gaeuman et al. 2016). The authors defined and evaluated several new 2- and 3-dimensional metrics that quantify various aspects of stream morphology, including metrics derived from the statistics of spatially distributed stream depths. In particular, a metric based on the range of depth percentiles within a stream reach (R^*) was found to correspond well with independent assessments of reach complexity, and a composite metric (χ^*) that incorporates R^* showed a moderately strong direct relationship (coefficient of determination = 0.53) with modeled juvenile salmon rearing habitat availability (Gaeuman et al. 2016). A follow-up study that presents correspondence between temporal changes in the range of depths in a stream reach subjected to repeated gravel augmentations and changes in two different measures of juvenile salmon habitat further support the hypothesis that depth variability is an important determinant of physical habitat quality (Gaeuman et al. 2019). The Gaeuman et al. (2016) report also argued that the extent of overbank inundation is a critical determinant of ecosystem function and proposed two inundation metrics to quantify it.

For the analyses of morphologic complexity presented herein, we follow Gaeuman et al. (2016) by adopting, with minor modifications, R^* to evaluate in-channel complexity and by examining width-to-discharge curves that depict how reach-averaged inundated width varies over a range of ecologically significant discharges. As originally presented by Gaeuman et al. (2016), R^* was originally defined as the average of the interquartile depth range and the interdecile depth range, normalized by the median depth. For this report, we adopt a slightly modified version of the original formulation introduced by Gaeuman et al. (2021), so that R^* is given by:

$$R^* = [(h_{75} - h_{25}) + (h_{90} - h_{10})] / (h_{90} + h_{10}) \qquad (3)$$

where h is a depth percentile given by the subscript and all depths are based on a reference discharge (Q_R) of 56.6 m^3/s. The empirical and theoretical reasons for this modification, as well as a detailed description of how the depth percentiles are obtained, can be found in Gaeuman et al. (2021).

Inundation widths and capacity

We computed reach-averaged inundation curves, in terms of average wetted width, for two sets of reach polygons – the seven stream segments corresponding to changes in maximum fisheries flow (MFF) discharges incorporated into the 2016 hydraulic model runs (Bradley 2016) and the 24 stream reaches defined by Gaeuman et al. (2016), which are here referred to as RC reaches (Figure 17). We did not compute average widths at rehabilitation site scale because defining limits of the overbank areas to be included becomes ambiguous at smaller spatial scales.

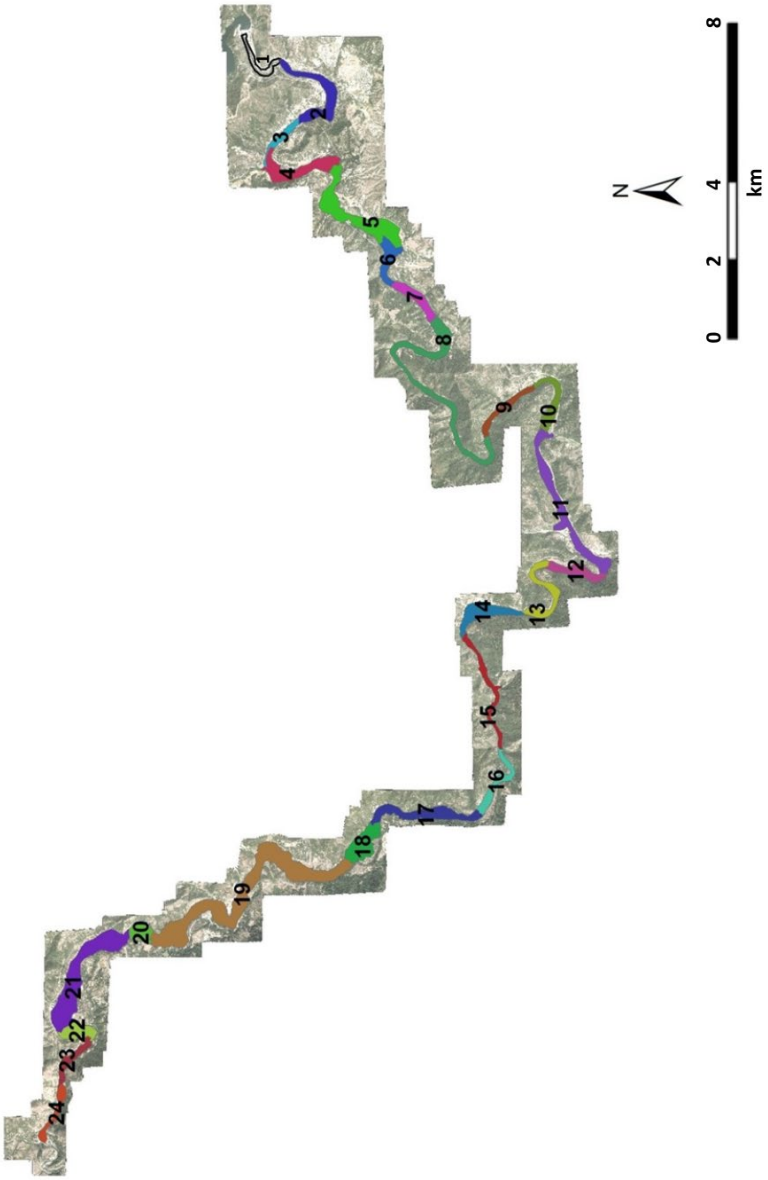

Figure 17. RC reaches of the Trinity River defined by Gaeuman et al. (2016). Reaches are numbered from Lewiston Dam downstream.

Figure 18 shows reach-averaged wetted widths for the seven MFF reaches plotted as functions of discharge (Q). All three graphs are plotted using axes with the same numeric ranges, making it immediately obvious that the rate at which inundated widths increase is close to three times greater near the upstream end of the study area (MFF reach 1 and 2) than in the downstream half (MFF reaches 5, 6, and 7), whereas the two reaches in between show intermediate rates of width increase. This result mimics the broad trend for decreasing habitat capacity with downstream distance displayed by the capacity curves described previously.

Regardless of their rates of increase relative to other reaches, average wetted widths within each of the MFF reaches increase most rapidly at low discharge levels as water spreads across the active channel bed. The curves tend to flatten as the active channel bed approaches full inundation at discharges ranging from about 10.6 to 25.5 m^3/s. Once the streambed is fully wetted, however, widths in most reaches continue to increase at a nearly constant rate through 170 m^3/s, the largest discharge displayed in the figure. Only Reach 1 displays a secondary flattening at about 99 m^3/s. Very little morphologic expression of a "bankfull" discharge at which flow would spread rapidly over a relatively flat floodplain surface is apparent in these curves. Among these seven reaches, the most notable deviation from a linear trend beyond the initial wetting of the streambed is the secondary flattening of the Reach 1 curve noted above. This, however, is opposite the effect expected of a bankfull threshold, which should cause the curve to bend upward. The curves for Reaches 5, 6, and 7 do show slight increases in slope at 141.6 m^3/s, but the magnitude of the increases is so small as to be of questionable significance.

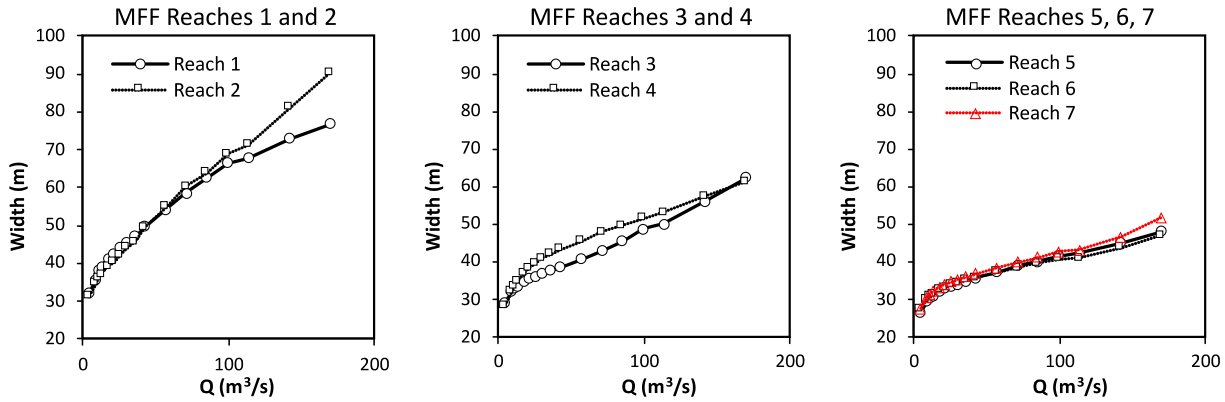

Figure 18. Reach-average wetted width to discharge curves for discharges of 4.2 through 170 m3/s in MFF reaches.

The lack of a clear bankfull signature is perhaps not surprising, as the upper end of the discharge range shown in Figure 18 is approximately equal to the mean annual flood near Lewiston Dam and substantially less than the mean annual flood in downstream reaches. This result indicates that the inflection points on the discharge to habitat capacity curves presented earlier (i.e. the apex of the habitat "dip" where the slope of the curve switches from negative to positive) do not correspond to floodplain inundation thresholds. Although it is not directly related to the habitat evaluations that are the topic of this report, it may be of general interest to the reader that plots of width to discharge curves extended to the largest permissible flow release

from Lewiston Dam under current operating rules (311 m^3/s, not shown) continue the essentially linear trend.

Plots of reach-averaged wetted widths for the 24 RC reaches show somewhat more variability than do the MFF reaches, but most reaches show the same general pattern with an initial rapid increase at the smallest discharges followed by an essentially constant rate of increase through 170 m^3/s (Figure 19). Curves with significant inflections to steeper slopes include RC reaches 3, 5, and 10, whose curves steepen to slopes of about 0.48, 0.57, and 0.39 $m/(m^3/s)$ beginning at discharges of 42.5, 42.5, and 142 m^3/s, respectively. Those reaches are among the few that Gaeuman et al. (2016) singled out as having unusually well-developed floodplains, noting that extensive terrace lowering was performed in RC reach 3 as part of the 2009 Sawmill rehabilitation project and attributing the relatively large floodplain area in RC reach 10 to a local lack of historical gold dredging activity. Similarly, the Lowden Ranch and Bucktail rehabilitation projects implemented in 2010 and 2015 involved extensive terrace lowering and floodplain development in RC reach 5. Inflections to slightly higher slopes at discharges near 113 m^3/s are also evident in a few other reaches, such as RC reaches 19 and 21 near the downstream end of the study area, but the general slopes of those curves are exceptionally low and even with the upturn the maximum local slopes remain less than 0.18 $m/(m^3/s)$.

As is the case with the MFF reaches, rates of increase in inundated widths with discharge are much greater in the RC reaches near Lewiston Dam than in the downstream reaches, with the maximum slope between 4.2 and 170 m^3/s (RC reach 4) being 4.5 times larger than the minimum slope (RC reach 18).

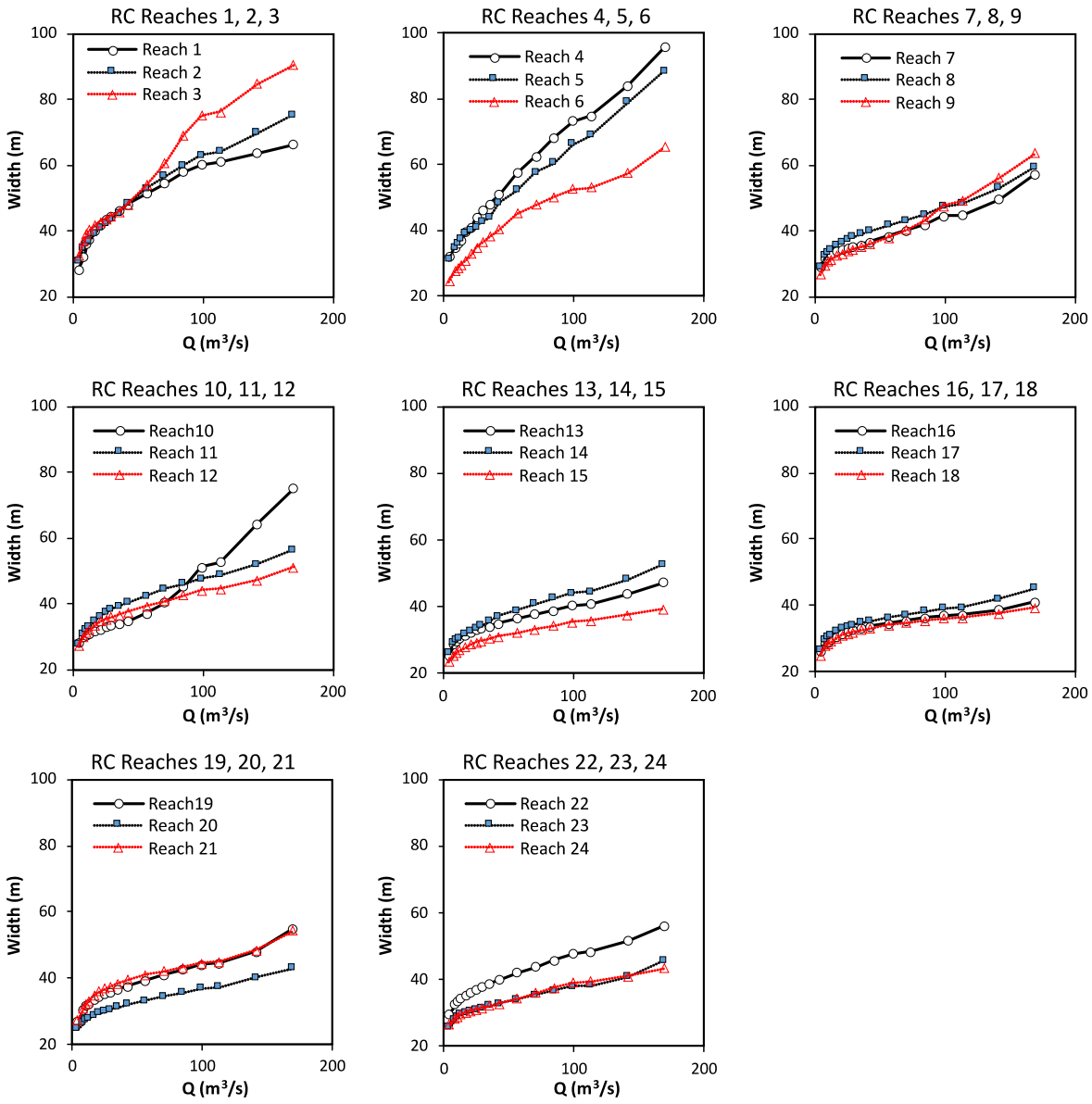

Figure 19. Reach-average wetted width to discharge curves for discharges of 4.2 through 170 m3/s in RC reaches.

Among our working hypotheses to be tested is that wetted width is a primary determinant of habitat capacity and could potentially even serve as a proxy for capacity. Wetted width, however, must either increase with discharge or remain constant, whereas fry capacity almost invariably starts out at a moderately high level at the smallest modeled discharge of 4.2 m^3/s and then decreases to a minimum when discharge is somewhere near 30 m^3/s. When plotted against width, fry capacity curves therefore take on a U or V shape with decreasing capacity values on the left limb and increasing capacity values on the right limb (Figure 20). The curves are skewed to greater or lesser degrees depending on the rate of width increases to the left of minimum capacity value relative to those on the right. Where the right-hand rates are greater, the curves are highly skewed, whereas similar rates on each side lead to more symmetrical U or V shapes. Presmolt curves assume shapes that are similar to fry curves, but the relative magnitude of

decreases observed on the left limb of presmolt curves tend to be smaller relative to changes on the right limb than for fry curves. In a few cases, presmolt capacity increases with discharge or remains essentially constant with increasing discharge throughout the full range considered. In addition to shape of the curves, Figure 20 highlights large variability of the range of wetted widths in different reaches. Interestingly, channel widths at the points of minimum capacity are relatively constant from reach to reach. For example, standard deviation of wetted widths at inflection points of fry curves for the 24 RC reaches (3.6 m) is just 9% of mean width at the inflection (39 m).

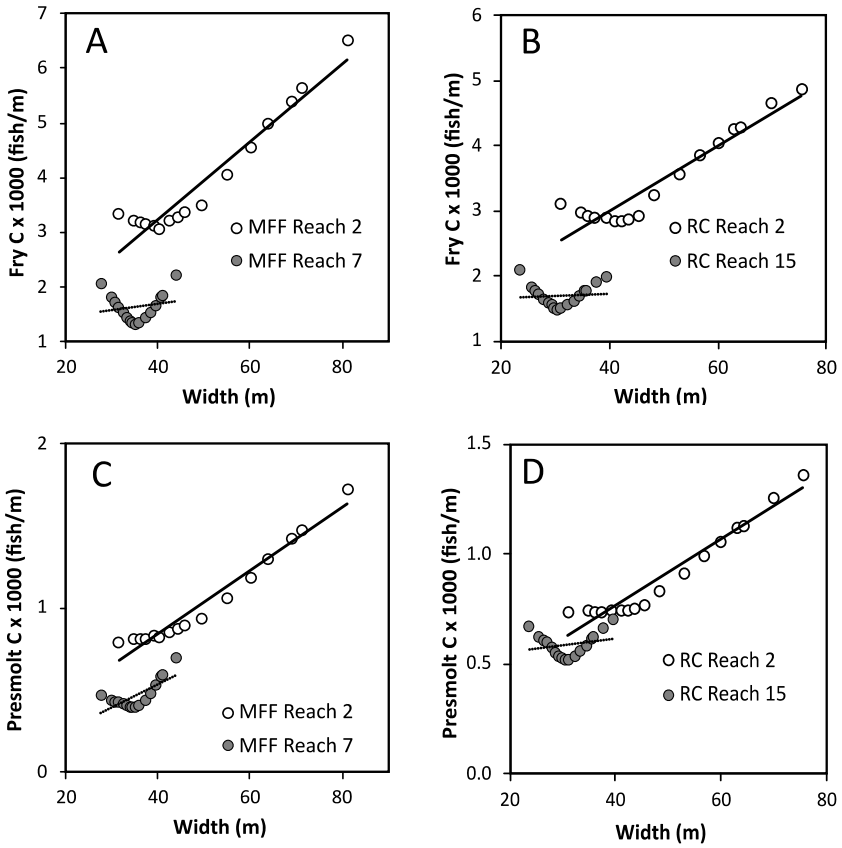

Figure 20. Plots of habitat capacity versus reach-averaged wetted width. Graphs are fry capacity in A) two example MFF reaches and B) two example RC reaches, and presmolt capacity in C) the same MFF reaches and D) the same RC reaches.

Although wetted width cannot represent the left limb of the capacity curves when capacity values are decreasing with discharge, width appears to have an almost 1:1 correspondence with capacity values on the right limb of the curve. When the left limbs of the capacity-to-width curves are removed, the remaining right limbs conform almost perfectly to a linear trend (Figure 21). Moreover, the slopes of the linear trends are remarkably consistent for fry and presmolt capacity. Slopes of trend lines fit to fry capacity data average 85 fish/m for each 1 m increase in wetted width for both sets of reaches, whereas slopes of presmolt trend lines average 27 fish/m for each 1 m increase in width. For MFF reaches, which are longer, standard

deviations in slope values for fry data are 13% of the mean and for presmolt standard deviation is just 8% of the mean. In the shorter RC reaches, standard deviations of slopes are about 25% of the mean values.

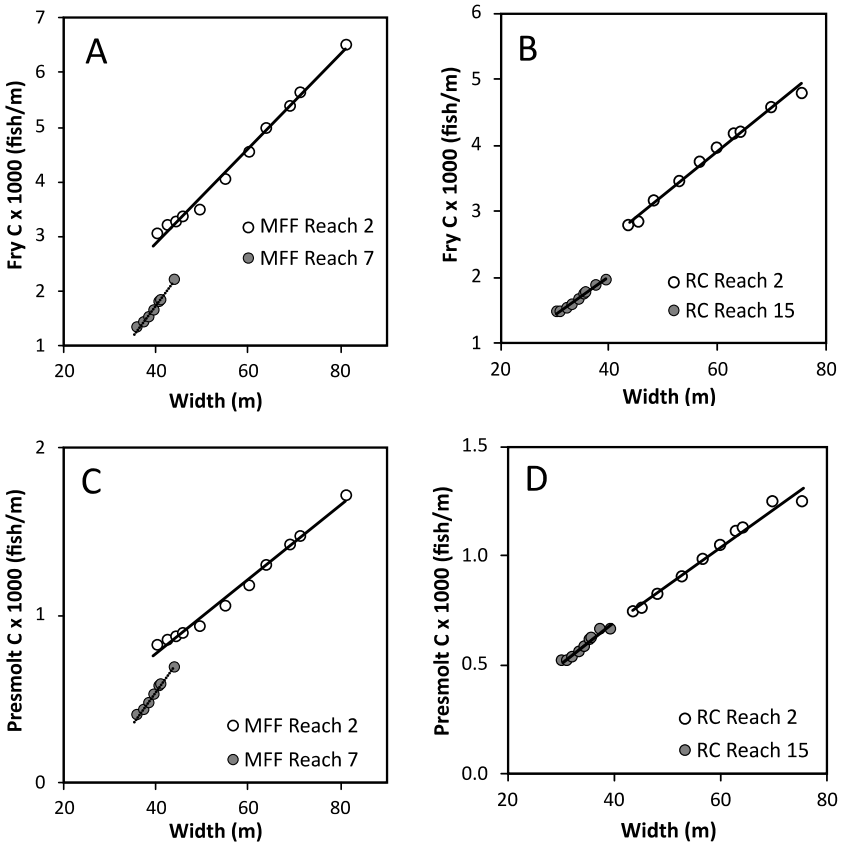

Figure 21. Plots of right limbs of capacity-to-width curves with linear trend lines. Graphs are fry capacity in A) two example MFF reaches and B) two example RC reaches, and presmolt capacity in C) the same MFF reaches and D) the same RC reaches.

The relatively consistent slopes displayed by right limbs of capacity-to-width data suggests that reach-averaged wetted width could serve as a metric of juvenile salmon habitat availability beyond the limits of the active channel bed. Intercepts of the fitted trend lines, however, vary from reach to reach because trend lines begin at a capacity value near the minimum value on the full curves. Trends of a given slope that begin at a smaller capacity value will obviously intercept the y-axis at a lower point. We hypothesize that starting capacity value at the left end of trend lines depends on topographic complexity of the streambed, which is essentially independent of conditions at channel margins and beyond.

Topographic complexity and capacity

Values of R^* computed for each MFF reach are tabulated in Table 5, and R^* computed for the 24 RC reaches are presented in Table 6 along with reach lengths and distances from Lewiston Dam.

As was the case for wetted width, *R** was not computed for rehabilitation site polygons because this metric is unsuitable for application at such small spatial scales. Boundaries of rehabilitation site polygons do not generally coincide with geomorphic units, so values of *R** would be heavily influenced by what portions of geomorphic units (e.g., riffle-pool or riffle-run sequences) spanning boundaries are included in the computation.

Table 5. Values of R* computed for MFF reaches.

Reach	Description	*R**
R1	Lewiston Dam to Rush Creek	1.24
R2	Rush Creek to Grass Valley Creek	1.37
R3	Grass Valley Creek to Indian Creek	1.04
R4	Indian Creek to Weaver Creek	1.09
R5	Weaver Creek to Browns Creek	0.99
R6	Browns Creek to Canyon Creek	0.95
R7	Canyon Creek to North Fork Trinity	0.94

Values of *R** for MFF reaches show strong correlations (Pearson's $r = 0.99$) with both fry and presmolt capacity computed for the reference discharge of Q_R = of 56.6 m^3/s (Figure 22). That flow level was selected for this comparison to match the reference flow level used in computation of *R**, and capacity values computed for that flow, hereafter referred to as reference capacity (C_R). Because the region inundated by Q_R encompasses regions inundated by all smaller discharges, Q_R is expected to also correlate with capacity values computed for those smaller discharges. We evaluated that expectation by plotting *R** against integrated area under the capacity curves between the lowest modeled flow level of 4.2 m^3/s and Q_R. Denoted as fry I_R and presmolt I_R, those integrated areas have units of number of fish/m per second. As these units have no physical significance, we omit them when discussing I_R. As shown in Figure 32, I_R values also show strong correlations with *R**.

Correlations between *R** and C_R, and between *R** and I_R for RC reaches are weaker than for MFF reaches but are nonetheless still significant at better than the 95% level (Figure 33). The RC correlations are presumably weaker than MFF correlations because RC reaches are much shorter. Because RC reaches sample a smaller spatial domain, a local section of stream with an unusual or anomalous morphology can more strongly influence values of *R** computed for the reach. One type of anomalous morphology that appears to generate much of the scatter in capacity to *R** relationships are pond-like features with uniformly low flow velocities. In such environments, flow velocities are found suitable for salmonid rearing, so capacity values depend primarily on the volume of the feature and distribution of cover within it. Factors that determine capacity are thus decoupled from topographic structure. *R**, which represents topographic variability in lotic environments, is notably different in its value of habitat in more lentic environments compared to the capacity model. Presence of these lentic environments therefore contributes to some of the scatter in *R** to capacity relationships, especially for shorter RC reaches.

Table 6. Values of R* computed for RC reaches defined by Gaeuman et al. (2016). Values of R* are based on Equation (4) rather than Equation (3), and so differ from values reported by Gaeuman et al. (2016). L = reach length, RK = river distance from Lewiston Dam to midpoint of the reach.

Reach	Name	*L* (km)	RK (km)	*R**
1	Tailwater Zone	1.90	0.80	1.17
2	Lewiston 1	3.37	3.59	1.30
3	Lewiston 2	1.27	6.10	1.13
4	Rush Creek Delta	2.39	7.87	1.42
5	Bucktail-Lowden	3.23	10.56	1.32
6	Trinity House Gulch	1.26	12.88	1.24
7	Upper Poker Bar	1.50	14.23	0.86
8	Poker Bar Canyon	7.67	16.95	0.97
9	Steel Bridge	1.94	20.62	1.01
10	Vitzthum	2.07	24.57	1.15
11	ICWC	4.25	28.84	1.06
12	Douglas City	1.81	31.83	0.96
13	Steiner	2.74	33.95	0.91
14	Goat Farm	1.96	36.18	1.06
15	Canyon	4.03	38.95	1.03
16	Lower Canyon	1.46	41.84	0.91
17	Evans Bar	3.18	44.61	0.88
18	Chapman Ranch	1.16	46.79	0.71
19	Junction City	7.69	51.17	0.96
20	JC Campground	0.79	55.48	0.96
21	Bigfoot	3.87	57.90	0.91
22	Limepoint	1.17	60.36	1.09
23	Elkhorn	1.58	61.74	0.88
24	NF Confluence	1.43	63.14	0.95

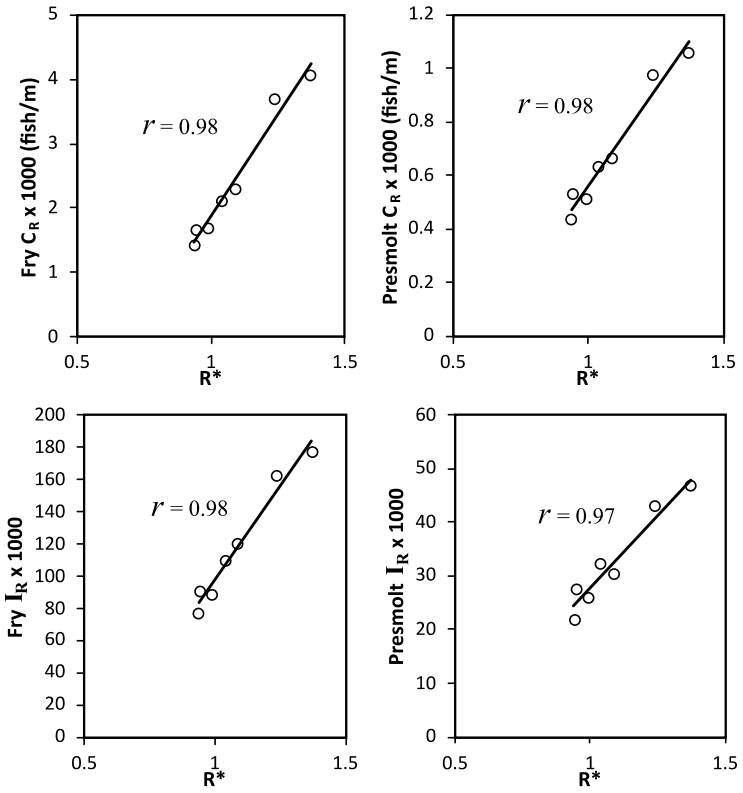

Figure 22. Fry (left) and presmolt (right) CR versus R* in MFF reaches (top row). IR (area under the fry and presmolt capacity curves between 4.2 m3/s and QR) versus R* in MFF reaches (bottom row).

For example, the largest values of C_R for both life stages in any RC reach correspond to RC reach 3, whose plotting positions are highlighted in red in Figure 23. RC reach 3 also attains the second largest value of fry I_R and third largest presmolt I_R among the 24 RC reaches. R^* computed for that reach, however, is relatively modest, such that RC reach 3 plots well above the regression lines shown in all figures, especially in the case of C_R for which RC reach 3 residuals are three times larger than for any other reach. Capacity values calculated for RC reach 3 are anomalously large because that reach encompasses the upstream half of a wide backwater pool that extends more than half a km upstream from a persistent delta at the confluence with Rush Creek (Figure 24). Flow velocities through that long, flat backwater pool remain small even at discharges well in excess of the reference discharge, resulting in large capacity values despite a general lack of topographic relief within the backwater zone. RC reach 3 attains its greater than average value of R^* only because the upstream half of RC reach 3 extends beyond the uniformly deep backwater pool to encompass a long shallow riffle that contrasts sharply with the pool morphology.

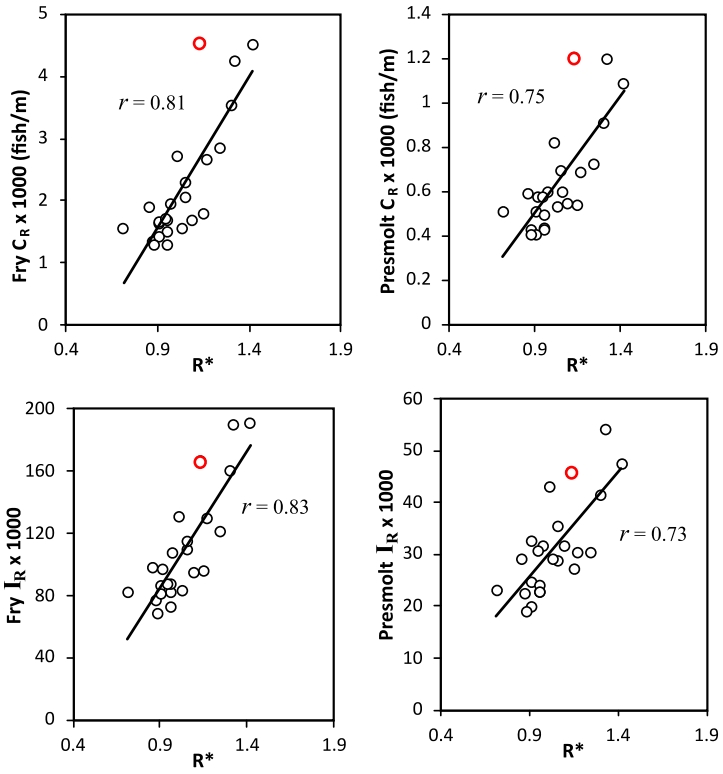

Figure 23. Fry (left) and presmolt (right) CR versus R* in RC reaches (top row). IR (area under the fry and presmolt capacity curves between 4.2 m3/s and QR versus R* in RC reaches (bottom row). The red symbol indicates the plotting position of RC reach 3, as discussed in the text.

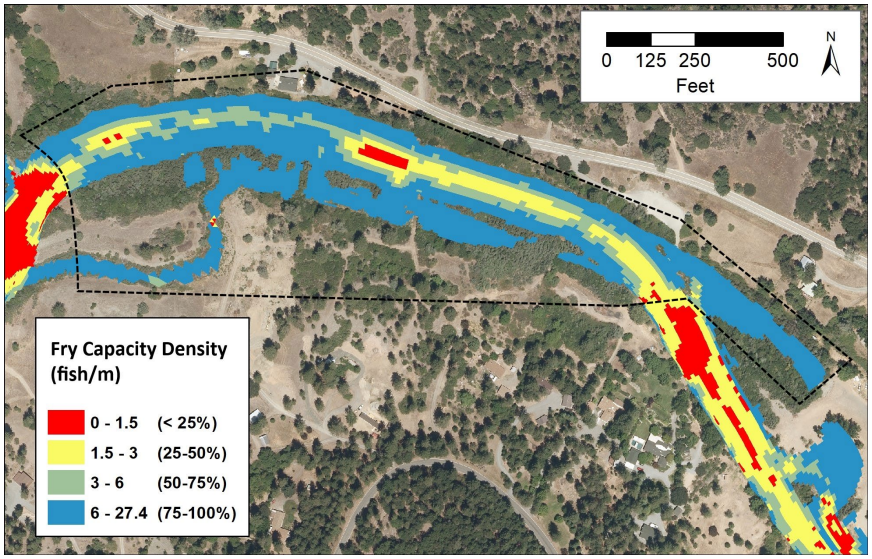

Figure 24. Rush Creek backwater pool area showing fry CR classified by quartiles. The majority of the backwater pool (outlined by dashed black line) has fry capacity densities in the upper quartile of values within the 40-mile TRRP focal area.

Wetted width and covariance among physical variables

Having introduced I_R for fry and presmolt capacity, it seems natural to also consider the integrated areas under reach-averaged wetted width curves. Following procedures used to derive I_R for capacity, we define I_{WR} as the area under the width-to-discharge between 4.2 m^3/s and Q_R. Linear regression between fry I_R and I_{WR} (Figure 25) show moderately strong to strong relationships. As both variables are calculated across the range of discharges less than or equal to 56.6 m^3/s, correlations show that wetted width is an important factor influencing fry capacity even on the left side of the capacity-width curves (Figure 20) where capacity decreases with increased width.

R^* is also directly correlated with I_{WR} for both sets of stream reaches (Figure 20). This result suggests that, all else being equal, channels with greater topographic variability tend to have wider active beds. This makes sense if one considers that topographic structures, gravel bars for example, occupy space in the stream that would otherwise be available for conveying water and that topographic irregularities of any kind contribute to hydraulic roughness.

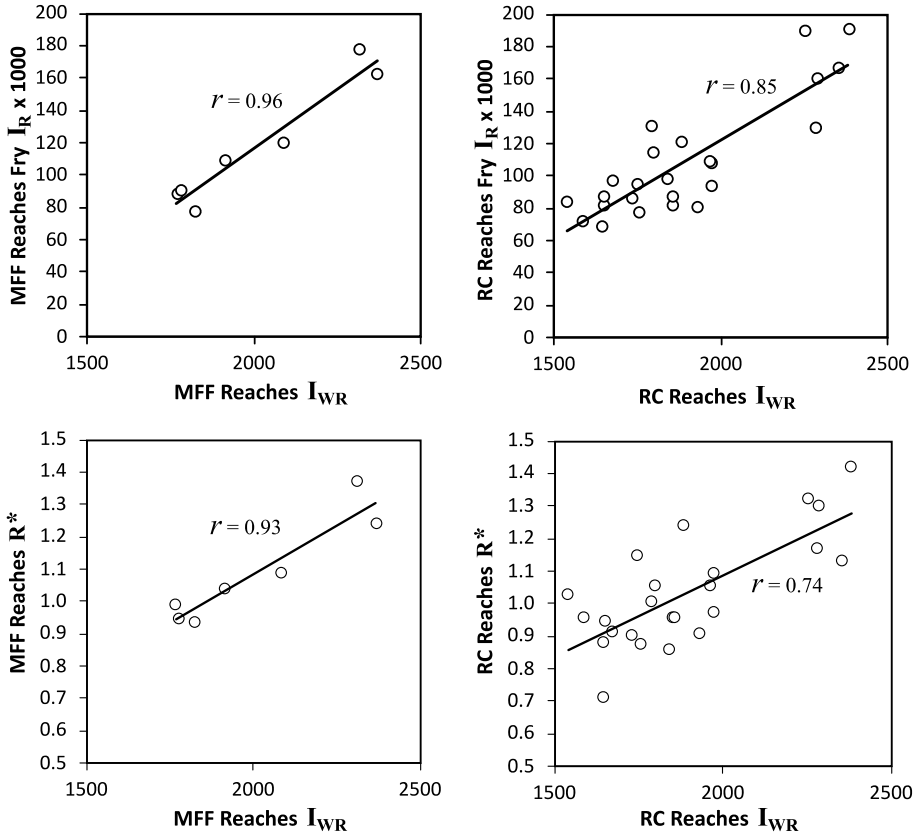

Figure 25. Plots of area under the fry capacity curves (IR) and R*as functions of the area under wetted width curves (IWR) in MFF and RC reaches.

Results presented above suggest that juvenile capacity is comprised of two components. The first component, which determines habitat availability at relatively small discharges, is a function of topographic complexity within a small region defined by the active channel bed. The second, potentially larger, component is determined by wetted width, which depends on morphology of the channel banks and adjacent floodplains. Where the boundary between those two components falls on the landscape and what its defining physical attributes are remain open questions. We begin to address those questions by evaluating the physical attributes incorporated into the habitat capacity metrics themselves.

Recalling that habitat capacity is a statistical model developed from observations of fish density in areas defined by flow depth, flow velocity, and distance to cover, we evaluated how each of those attributes relate independently to R^* and I_{WR} computed for MFF reaches via linear regression. For consistency with R^* we restricted analysis to values of mean depth, mean flow velocity, and proportion of wetted area with zero distance to cover (P_0) calculated at Q_R = 56.6 m^3/s. The most striking results of this analysis are strong correlations between P_0 and both measures of stream morphology (Table 7). As these three variables covary, all display similar inverse relationships with mean velocity and mean depth. The inverse relationships found between P_0 and the two hydraulic variables are as expected, given that cover is most often found along the channel margins where flow tends to be shallow and velocities are low. Likewise, the inverse correlations for depth and velocity with I_{WR} can also be anticipated, as the principle of continuity dictates that a wider flow can convey a given discharge at a smaller mean depth and/or a lower mean velocity.

The strong positive correlation between I_{WR} and P_0, however, is less predictable, because simply increasing the width of a trapezoidal channel will increase the average distance to the stream banks where cover is typically located. Instead, the relationship between I_{WR} and P_0 implies that wider reaches of the Trinity River are less likely to be trapezoidal in form. Instead, wider reaches often incorporate bars or islands that are emergent at baseflow but become inundated at moderate discharges. These topographic elements support riparian vegetation and can accumulate woody debris that become in-channel cover as discharge increases above baseflow.

Table 7. Pearson's r obtained from linear regression between listed variables for habitat capacity and complexity.

		Independent Variable	
Dependent Variable	P_0	Mean Depth	Mean Velocity
R^*	0.96	−0.85	−0.94
I_{WR}	0.93	−0.93	−0.96
P_0	--	−0.99	−0.79

R^* was explicitly developed to quantify this kind of topographic complexity, and its strong linear relationship with P_0 demonstrates that the distribution of cover over the riverine landscape is dependent on topography. It is instructive, however, to consider whether P_0 or R^* should properly be considered the independent variable in their relationship to one another. Cover, whether in the form of accumulations of woody material or live vegetation, tends to

develop where elevation of the stream bed is relatively high, such as on bar or along upper banks where hydraulic stresses tend to be low. On the other hand, presence of cover can dampen hydraulic stresses available for transporting sediment and lead to local sediment deposition, which can ultimately create topographic structures that increase bed relief. Rather than assigning one as being the causative factor and the other as being a response, it is undoubtedly more accurate to view them as interdependent attributes that evolve together. Although mutual dependence between development of vegetation and morphologic features is widely appreciated, explicit recognition of those interactions seems to introduce something new in the conceptual models that guide management of the Trinity River. Models codified in documents such as the Integrated Assessment Plan (TRRP and ESSA 2009) treat the concept of channel complexity as an independent physical attribute that exists in isolation from biological attributes such as riparian vegetation. Instead, vegetation near the active channel bed has often been perceived as a threat to topographic complexity that requires mitigation. Likewise, approaches to assessing juvenile salmon habitat tend to treat cover as an independent factor that has no relationship to topographic structure of the river. The tight relationships between presence of cover, topographic complexity, and habitat capacity suggest that these three environmental attributes are properly viewed as different expressions of a single landscape condition.

The above data also seem to indicate that the dividing line where habitat availability begins to increase in direct proportion to wetted width is located where the streambed and banks begin to support some level of riparian development. As flow encroaches onto surfaces of in-channel bars or creeps higher up bank slopes it begins to encounter vegetation, sparse perhaps at first but more fully developed as water stage rises. It is at that point when the definition of suitable juvenile habitat essentially becomes whatever is wet. The greater the topographic complexity, the greater the diversity of cover, and the lower the discharge at which that point is reached.

Objective 4: Evaluate the availability of habitat capacity within reaches given frequency and duration of flows during the critical rearing period

Habitat capacity with changing flow durations and annual flow regimes

While the first three objectives of this report allowed us to assess capacity spatially, we also sought to assess how capacity is affected through time with changing flow durations. We used daily flow duration curves from months January through May to assess how daily flow duration (and therefore capacity duration) is affected by differing accretionary flows. While some areas provide greater capacity than others over a fixed range of 4.2 to 99.1 m^3/s, we recognized that the highest capacities are typically associated with higher magnitude flows that occur over a small amount of time such that the high-flow habitat does not provide much ecological benefit for fish and may be overvalued. Additionally, we investigated how areas

farther downstream which experience minimum capacities associated with mid-range flows (i.e. habitat dip) undergo such conditions for longer durations due to dam-released winter base flows combined with accretionary flows from tributaries.

To illustrate the effect of differential hydrology on reach capacity, we plotted reach capacity (*C*) on the y-axis with daily average flow exceedance probabilities on the x-axis for each of the seven MFF reaches and their respective daily flow duration curves (Figure 26). We used daily flow duration curves of MFF reaches to relate corresponding flow-specific *C*. Because the capacity model provided estimates over a range of singular flow rates, capacity values were interpolated between flows with specified *C* estimates. This was done using a cubic spline interpolation function (R Core Team 2020), where 1,000 equally spaced points between 14 flow values from their minimum to maximum were estimated with corresponding *C* values. Interpolated *C* values were plotted on a secondary y-axis with corresponding *Q* (y-axis) as they occurred on a daily flow duration curve's (FDC) exceedance probabilities (x-axis). The capacity duration curve (CDC) for each sub-reach is depicted below in order from left to right, top to bottom as they occur in distance from Lewiston Dam. Each FDC is plotted at the same scale of Q. For each CDC, we used different scales of C between life stages but the same range of capacity within life stages for comparison of changes in capacity magnitude between reaches.

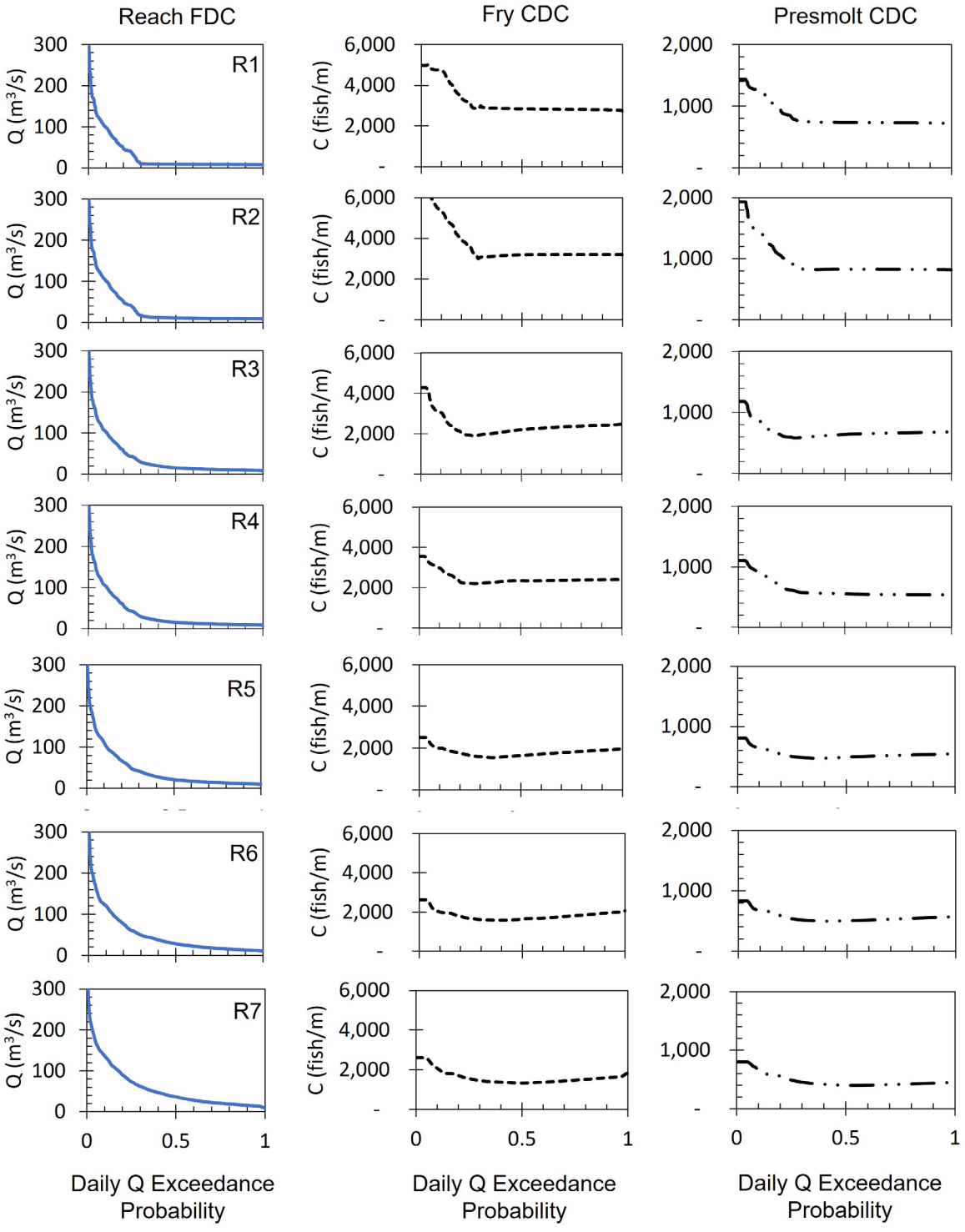

Figure 26. Daily flow duration curves (FDC) in MFF reaches R1 – R7 from top to bottom, left panel, plotted with their capacity duration curves (CDC). CDC's are the corresponding flow-specific fry (middle panel) and presmolt (left panel) capacities. Note change in scale of C between fry and presmolt life stages.

Figure 26 illustrates the relationship between capacity and flow duration probabilities in each sub-reach. While the MFF reaches illustrate the same general declining trend in overall capacity from upstream to downstream, as previously shown in Objective 1, it was clear how less frequent high flows make up only a small portion of capacity potential throughout the sub-reaches. Under current hydrology, capacity-rich flows on the far-left side of graphs occur infrequently, typically less than 30% of the time throughout the critical rearing period and generally in reaches closer to the dam. In general, both fry and presmolt *C* experience a positive relationship with *Q* during those higher flows occurring < 30% of the time. Despite fixing a range of flows in Objective 1 to more frequent rearing period flows (< 88% exceedance) throughout all sub-reaches, the flows in the lower end of that range represent a greater proportion of rearing capacity availability.

To reiterate temporal effects of flow on capacity, we evaluated capacity's response to annual flow regimes by plotting flow-specific capacity estimates over a given water year (October 1 – September 30). We plotted capacities as their specific flows corresponded with historical flow data over three water year types including Critically Dry (WY2020), Normal (WY2012), and Extreme Wet (WY2017) to illustrate how capacity changes throughout reaches under differential hydrology (Figures 27 and 28). We assigned capacity values using those interpolated from 14 capacity-flow estimates over 4.2 – 99.1 m^3/s, as done previously.

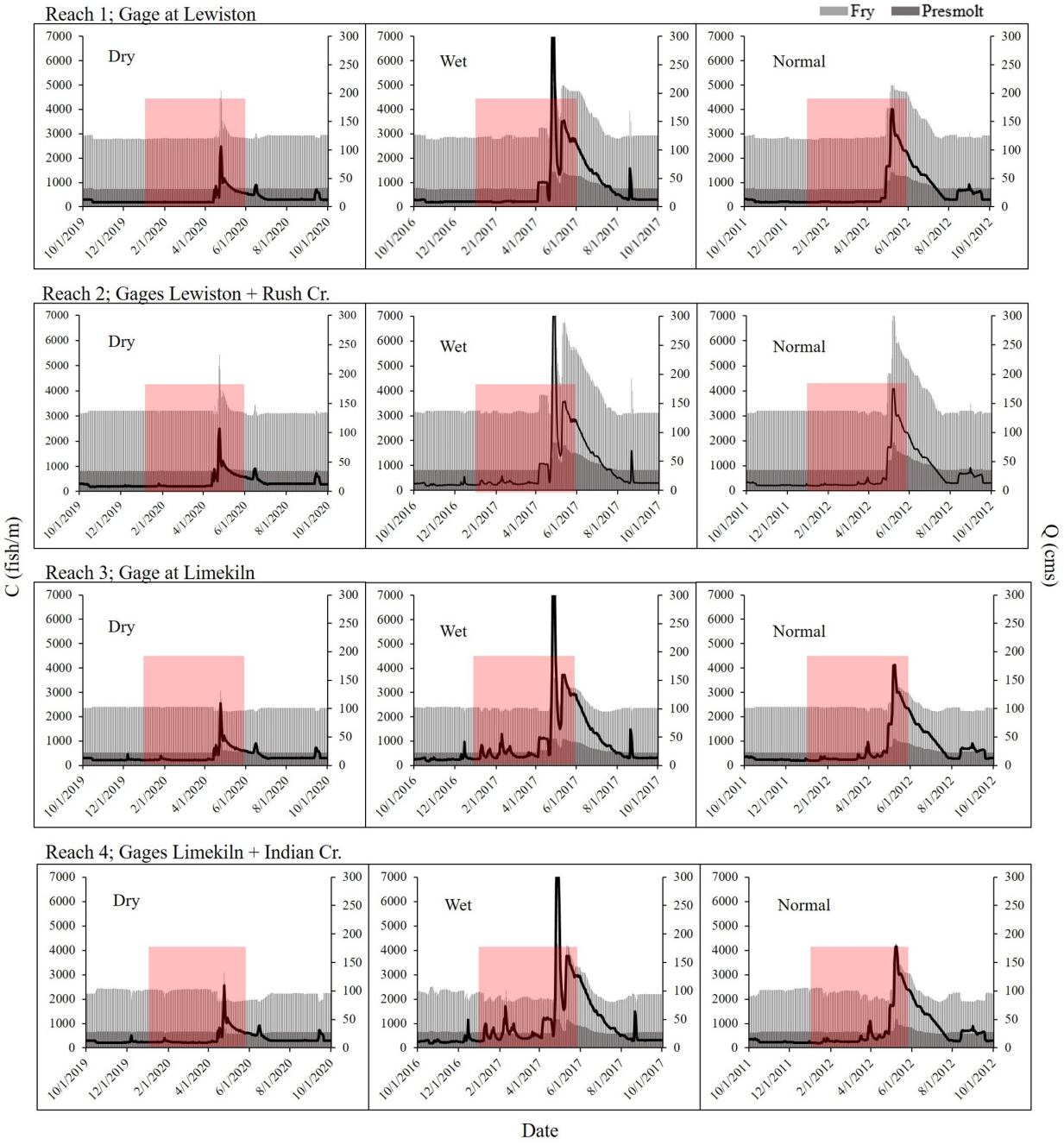

Figure 27. Capacity estimates for Chinook Salmon fry (lighter shaded area) and presmolt (darker shaded area) in MFF reaches R1 – R4 with flows from critically dry (WY2020, left), extreme wet (WY2017, center), and normal (WY2012, right) water years (solid black line). Red area indicates the critical rearing period from January through May.

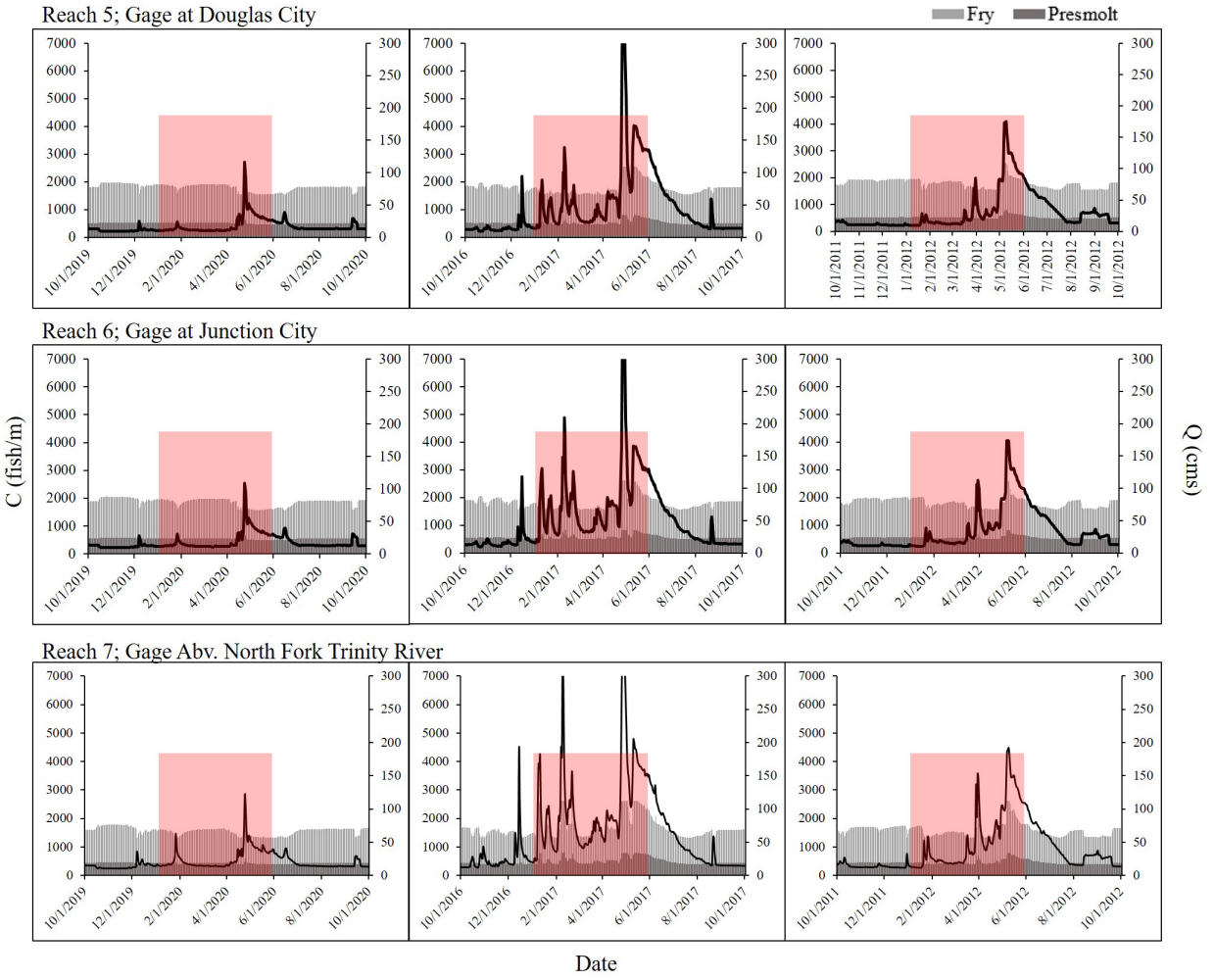

Figure 28. Chinook Salmon fry (lighter shaded area) and presmolt (darker shaded area) capacity estimates for MFF reaches R5 – R7 with flows from critically dry (WY2020, left), extreme wet (WY2017, center), and normal (WY2012, right) water years (solid black line). Red area indicates the critical rearing period from January through May.

Capacity is not cumulative, so an area's rearing capacity is only as great as its most limited capacity over a timing and duration that fosters ecological process (e.g. time of year and duration required for life stage success). Over WY2006 – WY2020, capacity availability within years has been determined by baseflow management for about 70% of the rearing period until the ROD flow release from mid-April, which accounts for about 30% of the rearing period and whose benefits can be seen in the 0 - 30% exceedance flows in all reaches (Figures 27 and 28). Because winter baseflow occurs during the Chinook Salmon fry life stage from January through the beginning of April, fry capacity is almost entirely limited to baseflow conditions, especially in the upper reaches where more abundant spawning is observed. It is likely that Chinook Salmon presmolts are the only life stage able to utilize rearing habitat that benefits from April flow releases, but that life stage is limited by bottlenecks in earlier life stages. Although greater flows occur more frequently downstream during the rearing period from tributary contributions, we found that capacity remains near minimums due to the broad habitat dip that occurs in these

reaches. As a result, throughout the entire restoration reach for the majority of the rearing period, flow-related habitat capacity is limited under current management.

To evaluate the influence of annual variation in discharge on physical habitat capacity over a broader geographic scale, we evaluated restoration reach-scale capacity as it occurs over each annual hydrograph during the available period of record (WY2006 – WY2020). This does not account for changes in channel form, as the only physical channel data available was for conditions during 2016. Therefore, this serves as an index of physical habitat availability relative to hydrologic conditions while holding channel form constant. We plotted daily average flows in annual hydrographs with correspondent capacity over the WY2005-WY2020 period of record, resulting in 112 annual daily capacity curves (ADCCs). Capacity values were summed across reaches at each daily flow occurrence. Those summed daily capacities were then weighted by proportional reach length, resulting in 16 ADCCs representative of capacity at the entire restoration reach scale, with Julian day on the x-axis and flow-specific capacity on the y-axis (similar to Figures 27 and 28). We then integrated the area (I) under those 16 curves and standardized that value relative to the maximum I value among the 16 curves to get I_N. The I_N values for each ADCC for fry and presmolt were plotted over time (Figure 29). There is a decreasing trend over the years in physical capacity in response to conditions of constant channel form and varying annual hydrology. The lowest values of ADCC I_N for fry and presmolt, respectively, were 17 – 21% lower than the maximum values of ADCC I_N. The maximum occurred at the beginning of the period in 2006, and the minimum occurred in two years near the end of the period, 2018 and 2020.

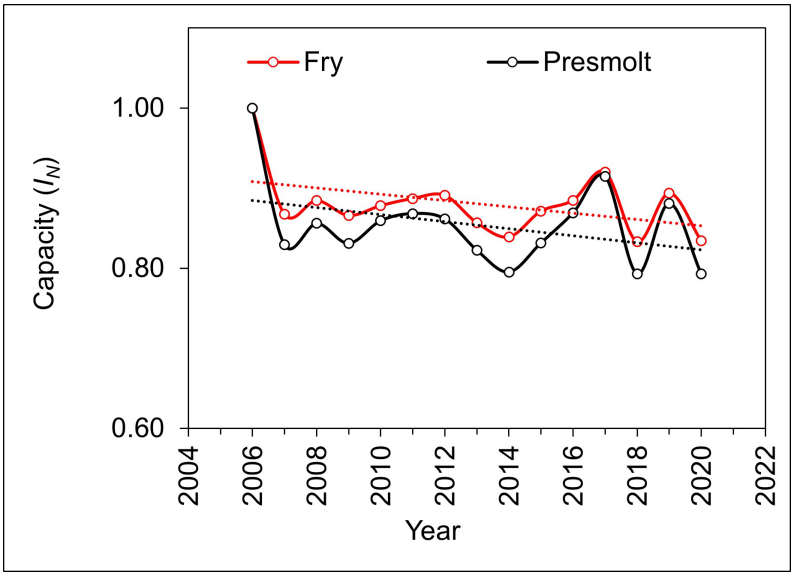

Figure 29. Time series and trend in juvenile Chinook Salmon physical habitat capacity from WY2006 – 2020 measured by area under the curve (I_N) of annual daily capacity curves (ADCCs).

Ecologically relevant flow durations

To further quantify differential hydrology and its effects on capacity throughout the restoration reach, we evaluated flow durations for consecutive days for areas associated with each stream gage. The Trinity River Channel Design Guide (HVT et al. 2011) states:

> *Pp. 15: "Winter Baseflow Magnitude-Duration-Frequency: The winter baseflows described in the previous section address "typical" values, but do not provide information on the frequency of duration for certain magnitudes. Inundation of certain features requires a duration component to provide valuable habitat. For example, if a feature such as a high flow scour channel is only inundated for 2 days during the January to April period, it would provide limited benefit to fry and juvenile salmonid rearing due to the short duration; however, if that same scour channel was inundated for 21 consecutive days, the additional duration would facilitate much more use of that habitat by fry and juvenile salmonids, and may also satisfy other objectives, such as primary and secondary productivity in the scour channel that would benefit fry and juvenile growth rates."*

Furthermore, consecutive-day duration curves can inform rehabilitation design with the following:

> *Pp. 16: "(1) biological thresholds can be compared to the frequency of certain flow durations…, and/or (2) translate typical winter baseflows… to a frequency-duration that can be compared to one or more biological criteria…."*

This is an important concept that we incorporated into evaluating capacity-flow relationships at the reach scale. Duration curves for 14 and 21 consecutive days of inundation were calculated and plotted for the period of record available from each gaging station during critical rearing months of January through May following methods from HVT et al. (2011) and USDA (2015) (Figure 30). To generate a duration curve representing the exceedance probability of 14 consecutive days of inundation, we calculated the minimum flow exceeded in a 14-day period preceding and repeated for each successive date over the critical rearing months for each year. These curves provided a way to translate consecutive days for flow duration into habitat capacity duration for a more ecologically relevant assessment of salmonid habitat rehabilitation. For example, rehabilitation sites upstream have features that provide greater habitat capacity when inundated at higher flowrates (>56.6 m^3/s), however those inundations occur for 21 consecutive days less than 10% of the time from January through May. Rehabilitation sites should be assessed not only in greater capacities over a fixed range of flows but also under flow conditions that occur for durations long enough to facilitate ecological process (e.g. subsequent life-stage success, macroinvertebrate recruitment), as suggested by HVT et al. (2011).

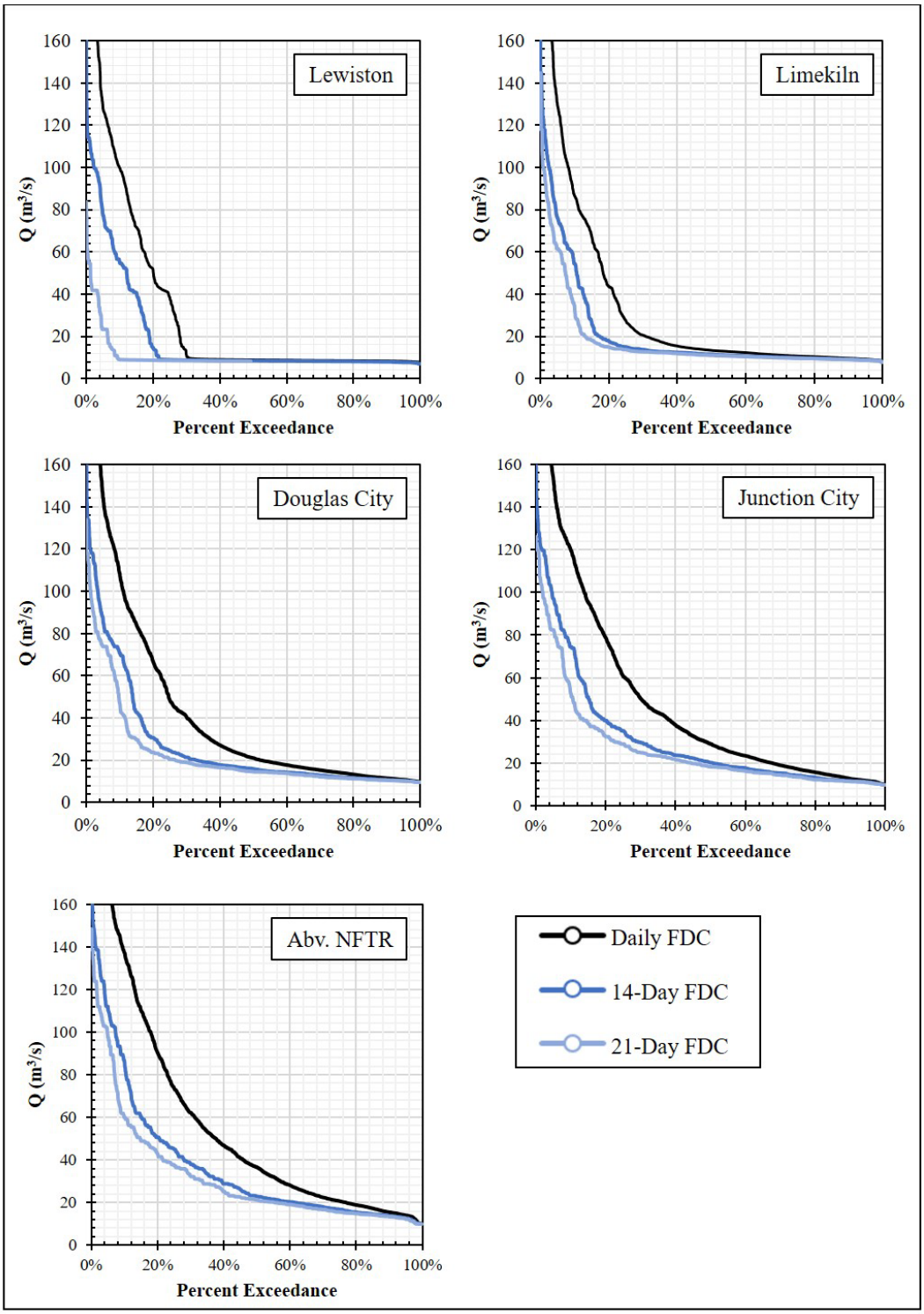

Figure 30. Flow duration curves (FDC) from five USGS stream gages in the Trinity River restoration reach during Chinook Salmon rearing period, January 1 through May 31. Daily FDC in black; consecutive day inundation for 14- and 21-day FDCs in dark and light blue, respectively. FDCs are generated using period of record (POR) from WY2005 – 2020. Data from 'Abv. NFTR' was incomplete in WY2005 and was limited to POR from WY2006 – 2020.

When comparing consecutive-day duration curves to each other, flow magnitudes decrease as more consecutive days of inundation are assessed. In general, consecutive-day flow magnitudes become greater and occur more frequently farther downstream. The 50% exceedance at the North Fork Trinity River gage site compared to at Lewiston gage site are 4.1 times greater in the daily flow duration curve and 2.5 times greater in a 21-day duration curve. Lewiston gage receives flows above 9.5 m^3/s (~335 cfs) about 30% of the time during Chinook Salmon rearing months. This area is inundated above 13 m^3/s about 10% of the time for a given 21 consecutive days in January through May. MFF reaches 3 and 4, associated with Limekiln gage, are inundated by flows above 20 m^3/s about 30% of the time on any given day and about 15% of the time for a given 21 consecutive days. Moving downstream to Douglas City and Junction City gages, MFF reaches 5 and 6 are inundated by flows greater than 20 m^3/s for any given day from January through May for 70% of the time and about 40% of the time for a given 21 consecutive days.

The consecutive-day flow duration analysis emphasizes how Chinook Salmon rearing capacity at a single flow, or even a set range of flows, is a limited way to assess habitat throughout the length of the restoration reach. In upper reaches of the restoration reach, habitat is limited to near baseflow but for 10% of the critical rearing period for the 21-day FDC. Greater capacity flows occur for 21 consecutive days only after April ROD flow releases from Lewiston Dam. This limits capacity for early life stages which subsequently limits production for following life stages. Juveniles may respond through density dependent dynamics of competition and movement, migrating to lower reaches to seek more suitable conditions. While lower reaches experience increased durations of inundation, the hydraulic conditions are mired within the habitat dip in those reaches, leaving rearing options suboptimal throughout the restoration reach over the critical rearing period. These consecutive-day FDC's may help managers understand not just the spatial distribution of capacity but also the temporal availability, which are both important aspects for juvenile salmonid habitat use.

Habitat capacity response to increased winter baseflows

In response to identifying physical habitat capacity limitations related to flow, we quantified hypothetical changes to capacity from alternative dam-released winter baseflows. Interpolated flow-specific capacity estimates (C) and daily FDC's for scenarios of increases in winter baseflow (Q_{base}) magnitude were applied to the WY2005 – 2020 period of record. Knowing that baseflow management occurs for about 70% of the days during the rearing period and that Q_{base} is managed at 8.5 m^3/s (300 ft^3/s), we expected 8.5 m^3/s to occur around the 30% exceedance probability at the Lewiston gage. However, we found variations in baseflow releases throughout all years from January to mid-April, most notably from 1 Jan – 17 Feb 2006 when there was a large safety of dam (SOD) release. On average, flows released during January through mid-April from 2005 – 2020 was 10.6 m^3/s, which is substantially greater than the expected 8.5 m^3/s for Q_{base}. When we eliminated the flows from the early 2006 release, average Q_{base} was 8.7 m^3/s (SD 0.8 m^3/s). We acknowledge that these variations are likely due to lesser

SOD releases and normal variability of dam operations. However, baseflow variations affected the Q_{base} magnitude for the exceedance flows from which we calculated scenarios of capacity response to increased Q_{base}. The actual 30% exceedance flow calculated at Lewiston in the FDC is 9.5 m^3/s (335 ft^3/s). For the purposes of quantifying habitat capacity's response to increased winter baseflows, we evaluated scenarios of increased Q_{base} magnitudes starting from a Q_{base} of 9.5 m^3/s.

At Lewiston, if the Q_{base} is 9.5 m^3/s during the critical rearing period of January through May, then increasing that baseflow would in turn increase all exceedance flows downstream. For example, increasing Q_{base} by 33.0 m^3/s would change the Q_{base} at Lewiston to 42.5 m^3/s (Q_c). This would also add 33.0 m^3/s to the exceedance flows in each reach downstream, whose values were previously quantified with the daily FDCs (Figure 2). We repeated iterations of increased baseflows defined in Table 8. Understanding that baseflows determine availability of juvenile capacity starting from the fry life stage, we calculated the percent change in fry capacity over the entire restoration reach from Q_{base} to Q_a, Q_b, and Q_c (Table 8, Figure 31). After calculating increased daily flows and corresponding C for each MFF reach, we summed C among all exceedance flows across sub-reaches proportional to their respective sub-reach length within the entire 64 km restoration reach. This essentially is a combination of those previously calculated individual MFF reach CDCs in Figure 26, weighted by MFF reach length. We plotted restoration reach-scale capacity duration curves (CDCs) for each baseflow alternative, calculated the basal rectangle (I_{Base}) where height was determined by C_{min}, calculated integrated area under those curves (I_D), and used the difference in $I_D - I_{Base}$ to calculate the percent change in I_D from Q_{base} (Table 8, Figure 31). In this way, we isolated the effect of flow management for each reach and reduced the relative effect of channel impairment, represented by C_{min}.

This analysis used interpolated capacity estimates from 4.2 to 99.1 m^3/s to produce capacity duration curves. As a result, all the CDCs in Figure 31 are flattened and converged at their start. Recognizing that iterations of increases in baseflow result in greater flow magnitudes than 99.1 m^3/s, we chose to maintain this magnitude threshold as higher flows would still be relatively infrequent. It is also unlikely springtime ROD flows would remain as they were in historical record due to limited water volume, but rather would likely be reallocated from spring release volumes to occur earlier in the year. Furthermore, because this analysis is mostly aimed at addressing bottlenecks in capacity at more frequent flows, the effect of including capacity values associated with less frequent flows where capacity is relatively abundant removes emphasis from the point of this analysis.

Table 8. Capacity response to flow durations from increased baseflow alternatives show an estimated change in capacity across the entire Trinity River restoration reach.

Baseflow Alternative	Q (m^3/s)	I_D	I_{Base}	I_D - I_{Base}	% change from Q_{base}
Qbase	9.5	2213	1935.4	277.1297133	0%
Qa	14.2	2188	1931.067	256.9326441	-7%
Qb	28.3	2191	1909.108	281.8922663	2%
Qc	42.5	2316	1987.997	328.0034732	18%
Qd	56.7	2494	2148.182	345.8176625	25%

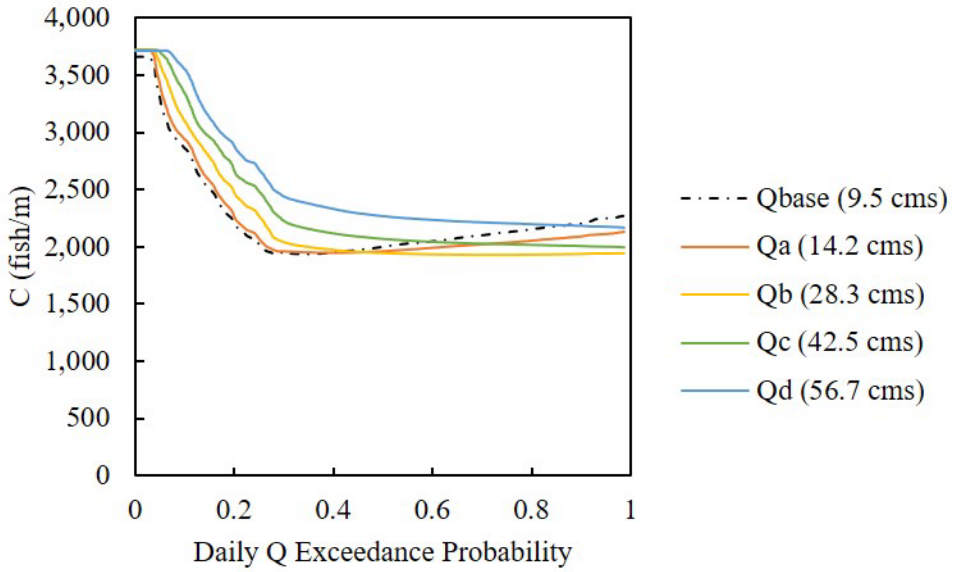

Figure 31. Chinook Salmon fry capacity duration curves for the entire Trinity River restoration reach where flow specific capacity is related to daily flow duration over current baseflow management (Q_{base}) and alternative increased baseflows (Q_a – Q_d).

With channel conditions in 2016 throughout the entire restoration reach, fry I_D decreased with an increase in Q_{base} to 14.2. A positive change is seen with an increase in Q_{base} to 28.3, 42.5 and 56.7 m^3/s, where fry I_D increases by 2%, 18% and 25%, respectively. Increasing baseflows to a level near 42.5 m^3/s or more would be a restoration reach-scale management strategy to help alleviate the winter rearing capacity bottleneck by creating greater habitat capacity throughout the restoration reach for longer durations over the rearing period. We recognize that static flow rate, analyzed here, during a time of year when there would naturally be runoff events of varying magnitude may be unrealistic. However, our estimates of increased capacity from a fixed increase in baseflow are meant to provide insight into potential capacity benefits with a relatively simple change in management.

Discussion

Objective 1 of this report found that reaches with similar hydrology and sediment regimes also have similar trends in habitat capacity. In Objectives 1 and 2, we found a negative trend between capacity and distance from dam where in general reaches and sites farther downstream have less capacity and experience habitat dips over a broader range of flows. Objective 3 found channel and floodplain planform important variables capable of explaining differences in habitat capacity with variation in flows. Finally, we found in Objective 4 how capacity is limited by flow timing and durations that change from upstream to downstream areas of the restoration reach.

Objective 1: Evaluate Chinook Salmon rearing habitat capacity for areas that have received mechanical rehabilitation and those that have not

The capacity to flow relationship was distinct between seven hydrologically similar Maximum Fisheries Flow (MFF) sub-reaches. This suggests similar physical limitations to capacity within those sub-reaches and that rehabilitation effectiveness can continue to be evaluated among those reaches. Rehabilitated areas had greater capacity than non-rehabilitated areas in sub-reaches from Rush Creek to Canyon Creek. MFF reach 2, from Rush Creek to Grass Valley Creek, had the greatest habitat capacity throughout the entire restoration reach. This sub-reach includes three rehabilitated areas with the greatest habitat capacity per river length, little to no habitat dip in the capacity to flow relationship, and the greatest proportion rehabilitated reach length (60%) of the seven MFF reaches. Despite a similar proportion of rehabilitation reach length between MFF reach 2 (60%) and reach 7 (58%), however, we found capacity was less in reach 7 than in any of the other MFF reaches. Capacity in MFF reaches was limited where channel settings are confined from either canyon geomorphology or anthropomorphic impacts within the valley.

Objective 2: Evaluate Chinook Salmon rearing habitat capacity at rehabilitation sites

Rehabilitation sites with the smallest values of minimum capacity and broadest habitat dips were typically areas with narrow, single-threaded channels that had little connection to floodplain or margin habitats, including most sites in reaches with incised or confined planform settings throughout the lower half of the restoration reach (MFF reaches 5, 6, and 7). One exception farther upstream was in MFF reach 3, but most of this reach is confined to a canyon setting where lateral habitat is limited. Site-scale features that contribute high capacity values became inundated at low-moderate flows and have side channels, floodplains, backwater areas, ponds, and areas with vegetative cover. Habitat capacity was greatest in MFF reach 2 mostly due to the Upper Dark Gulch and Bucktail rehabilitation sites. Upper Dark Gulch provides floodplain connectivity at low to moderate flows. An off-channel pond feature in Bucktail has low-velocity conditions suitable for fry and presmolts at low flows where other sites were typically lacking. Design features that inundate at lower or more frequent flows appear to increase minimum

capacities seen in the habitat dip throughout site and reach-scale evaluations. Minimum fish capacity at Bucktail was seen over a similar range of flows (~20 – 37 m^3/s) with a habitat mapping methodology used by Boyce et al. (2020). Upper Dark Gulch, Bucktail, and Lowden Ranch in MFF reach 2, Sven Olbertson and Sawmill in MFF reach 1, and Lower Indian Creek in MFF reach 4 have the greatest relative capacity (I_N) for fry and presmolts of all 24 sites evaluated. These top six sites all have minimum fry capacities (C_{min}) around 3,000 fish/m or more, whereas fry C_{min} at other sites range from 1,000 fish/m to 2,500 fish/m. The habitat dip has been corrected at these six sites with rehabilitation, and C_{min} occurs at or near the lowest flow modeled.

Objective 3: Evaluate physical channel metrics related to habitat capacity at multiple scales

We suggest physical habitat capacity responds to two distinct physical components of planform. One component is a function of topographic complexity within a region defined by the active channel bed and a second, potentially larger, component depends on planform conditions beyond the active channel bed. The differing behavior of the capacity to wetted width curves left and right of C_{min} show the dynamics that determine physical habitat within those areas of the fluvial landscape are fundamentally different. Within the extents of the active channel bed, the region where most water and bedload sediment is conveyed, habitat tends to be inversely related to increases in wetted width with discharge due to relatively low flow velocities that accompany small discharges. As discharge increases from near zero, the rate of increase in the extent of inundation is greater than the rate of increase in the depths and velocities of the flow, and juvenile habitat increases in abundance. As discharge continues to increase and the active bed approaches full inundation, flow depths and velocities begin to increase faster than the inundation extent, and the availability of fry and presmolt habitat within the extent of the active channel bed declines to a minimum. As the extent of inundation continues to expand beyond the active channel bed, flow begins to interact with bar slopes, stream banks, and other features of the channel margins that offer much greater structural variety than the mostly barren gravel and cobble found within the limits of the active channel. At that point, past the habitat minimum represented by the habitat dip, inundation extent and habitat capacity become highly positively correlated.

The apparent inverse relationship between low-flow habitat and increases in wetted width described above vanishes when different reaches are compared, as opposed to different discharges within a single reach. At the inter-reach scale, greater wetted widths are positively correlated with greater habitat capacities across the full range of discharges. In short, reaches that start out wider at the lowest flows and/or grow wider at a faster rate with increasing discharge provide more habitat than reaches with less wetted width. Additionally, the two physical variables presented appear to be interrelated, as reaches with greater wetted widths at discharges up to and including the reference discharge of $Q_R = 56.6$ m^3/s also tend to display greater topographic complexity, as measured by R^*.

The negative relationship found between capacity and downstream distance from Lewiston Dam can be explained in terms of physical differences between upstream and more

downstream reaches. We found decreases in both inundation width and channel bed topographic relief as measured by R^* in reaches farther downstream, and both of those variables were shown to be linked to capacity. The restricted, topographically invariable conditions in areas farther downstream provide minimal capacities at a wider range of flows for longer durations. This is likely due to the incision and entrenchment symptomatic of valley-scale mining activities and associated tailing piles combined with reduced flood magnitudes from dam and diversion operations, but the causes of topographic conditions have yet to be directly evaluated.

Objective 4: Evaluate the availability of habitat capacity within reaches given frequency and duration of flows during the critical rearing period

Relating flow-specific capacities within reaches to more frequent flows provided another lens through which to assess habitat capacity and can inform how rehabilitation design and flow release strategy coincide. The capacity duration relationship illustrates how availability of habitat capacity at the reach scale is a result of its more frequent flow durations. Accordingly, we found that flow-driven capacity bottlenecks exist within-years in the upper end of the restoration reach from winter baseflow magnitude and timing, and in the lower end of the restoration reach from flow durations sustained near minimum habitat capacity because of additional accretionary flows.

Physical habitat capacity decreased by 21% in 2020 from to 2006 in response to annual hydrology and constant channel conditions. Physical habitat availability being equally dependent on channel form and hydrologic conditions means that it is not currently possible to clearly state any trends about the availability of physical habitat during this period, and it is highly likely that the true availability of habitat to rearing juvenile Chinook Salmon in the restoration reach would not have a significant trend from WY2006 to WY2020 due to opposing forces of channel rehabilitation and poor hydrologic conditions. However, without channel rehabilitation, it is almost certain that a decreasing trend in habitat would have prevailed due to the influence of drought. Physical habitat rehabilitation sites are likely compensating for observed negative population pressures such as reduced fecundity or adult abundance (Pinnix et al. 2022, in draft), as well as water availability, drought, and flow management that prevent fully realized benefits from habitat rehabilitation sites.

An important distinction in capacity's response to changes in baseflow is that increases in flow magnitudes up to around 28.3 m^3/s would actually decrease overall capacity in the restoration reach. The negative response to increased flows is a result of maintaining flow conditions around capacity minimums in the lower reaches. Responses vary between sub-reaches due to their different relationships between capacity and flow with increases occurring in the upper reaches, but from a management perspective, it is most useful to consider flow changes at the entire restoration reach-scale. Changing flow release strategies simply with a fixed increase in baseflow management to 42.5 m^3/s or greater would increase current daily exceedance habitat capacity throughout the restoration reach by ~18% or more during the rearing period. While we chose to evaluate the entire period and did not do water year specific analysis due to the low and differential sample sizes of water years from 2006-2020, it is logical that increases to baseflows

would offer greater benefit under wet hydrology by overcoming the habitat dip more frequently, and could possibly cause decreases under dry hydrology by pushing lower reaches deeper into their dips. Potential increases in habitat capacity in lower reaches, where capacity is lacking compared to the capacity-abundant upper reaches, may be of critical importance as restoration of this area is scheduled to take a decade or more. We would also like to point out that all channel rehabilitation activities since 2016 have occurred in MFF reach 6 and include many of the largest projects (measured by cubic yards of earth moved) that the TRRP has ever completed (Sheridan Creek, Deep Gulch, Chapman Ranch, and Dutch Creek sties) (Gaueman et al. 2021). Capacity is likely underrepresented in this area at the time this report is being completed. Additionally, change in flow management would take greater advantage of rehabilitation efforts already completed thereby increasing their value.

Recommendations for future habitat assessments

Because this report was opportunistic and not based on a sampling design that addressed specific hypotheses, our mostly qualitative assessments were an exploratory effort that generated hypotheses. We found that not only is it important to improve physical salmon habitat but also to provide habitat with flow timing and durations that support ecological process. Ecologically relevant flows and their relationship to habitat availability should be further investigated with consecutive-day flow duration analysis and verifying appropriate consecutive-day thresholds. Furthermore, trends in physical limitations to capacity throughout specific sub-reaches are an important consideration in rehabilitation assessment and design. We hypothesize therefore that different restoration techniques are more appropriate for reaches closer to the dam versus reaches farther downstream: techniques in upstream reaches with wider valley extents should include features that provide hydraulic complexities at elevations inundated by more frequent flows, such as at Sawmill, Lowden Ranch, or Bucktail Ranch, whereas techniques downstream should focus on widening of the active channel via removal or consolidation of mining tailings.

In addition to rehabilitation efforts, flow management may look to change timing, duration, and magnitude that would support greater habitat capacity throughout the critical rearing period as the channel and its flow to habitat relationship are altered. We hypothesize that changes to flow management may provide the fastest and most effective action to increase habitat capacity at the time of year when juvenile Chinook Salmon are most abundant within the restoration reach. In addition to quantifying changes from fixed increases in baseflow, it may be worthwhile for future habitat assessment efforts to quantify capacity response to more variable winter flow management that mimics natural seasonal flooding using 14- or 21-day CDCs.

While the capacity model highly values low-velocity areas found in pond or backwater features, R^* deviated from that valuation due to the relatively smooth topography found in such large, lentic areas. This was empirically observed in the Rush Creek backwater area, but there are other similar backwater habitats such as Society Pool, Indian Creek Pool, and Bagdad, to name a few. This deviation should make us scrutinize how we value large areas of extremely low velocity. Other studies have shown that habitat suitability criteria (HSC) approaches which relate

physical habitat metrics to habitat use are prone to over prediction of suitability at the lowest velocities due to undervaluing energetic intake benefit of moving water (Rosenfeld and Ptolemny 2012, Hayes et al. 2016, Wheaton et al. 2017, Caldwell et al. 2018, Naman et al. 2019). The capacity model was developed in the lotic systems of the Trinity River and did not specifically account for sampling in lentic floodplain areas. Because capacity is calculated on the 95th percentile of observed fish density for a given habitat characteristic, it would not capture the differences between lentic and lotic environments; instead, it would attribute the more food-productive environment to the physical attributes of the lesser. We hypothesize that if the Trinity River capacity model does over-predict capacity at the lowest velocities, overall capacities would be lower than predicted at the lowest modeled discharges due to rate of increase in extent of inundation being greater than the rate of increase in depths and velocities.

While we assessed changes in physical habitat through spatial and temporal extents, we recognize that habitat is not only composed of physical characteristics. For example, the capacity model does not account for differences in temperature. Studies have shown that temperature is a driving factor of production and life history diversity in streams that can override most any other habitat requirements for juvenile salmonid growth and survival (Sullivan et al. 2000, Olden and Naiman 2009, Petty et al. 2013, Weber et al. 2014). A capacity model based on physical variables may overpredict capacity in areas with unsuitable temperatures. The S3 fish production model uses a 1-D longitudinal temperature model to inform a growth and disease sub-model (Perry et al. 2018a) and provides excellent information for flow actions, but to assess rehabilitation site design and effectiveness 2-D or 3-D temperature modeling would be required. We hypothesize that temperature and food availability are additionally important gradients of habitat quality and should be incorporated into future assessments of restoration action to improve habitat. Combining our existing hydrodynamic models with 2-D temperature and net rate of energy intake models to evaluate proposed management actions could provide a more complete synthesis of juvenile rearing habitat conditions, the potential for salmonid production, and ultimately the ecological capacity for self-renewal in the Trinity River restoration reach.

Conclusion

This habitat synthesis developed a better understanding of habitat capacity in rehabilitated areas, how capacity is related to flow and flow durations at reach and site-scale, physical metrics as covariates of capacity, and how habitat capacity changes with accretionary flows and dam release throughout the Trinity River restoration reach. Habitat capacity responded similarly to flows among reaches with distinct hydrology, and we identified where rehabilitation has increased juvenile salmon capacity and where it has not in those reaches. There was a general trend of declining capacity at the reach and rehabilitation site-scale with distance from Lewiston Dam. We found topographic complexity of the active channel measured with a novel metric, R^*, to be highly correlated with capacity at low to moderate flows. As flowrates increase, capacity responded positively to changes in wetted width, which inundate riparian vegetation and channel margins, and could serve as a potential proxy for capacity at flow stages beyond the

active channel. Going beyond physical determinants of capacity, we found it meaningful to evaluate capacity not only spatially but also temporally by quantifying changes with flow durations throughout the rearing period. Under current management, winter baseflow determines capacity during the fry life stage throughout the restoration reach because it's timing spans that of the typical Chinook Salmon fry life stage. Capacity is limited downstream from the Weaver Creek confluence where baseflow dam releases combined with tributary accretions produce long-duration flows that keep capacities near their minimum values over most of the juvenile salmonid rearing season. In conclusion, physical and biological conditions interact and change through time and space, so habitat capacity should be evaluated for its potential through timing and duration of its spatial extent.

Literature Cited

Alvarez, J., D. Goodman, A. Martin, and N.A. Som. 2013. Estimation of Age-0 Chinook and Coho Salmon Rearing Habitat Area Within the Restoration Reach of the Trinity River at an Index Streamflow-Annual Report 2011. U.S. Fish and Wildlife Service. Arcata Fish and Wildlife Office, Arcata Fisheries Technical Report Number TR 2013-18, Arcata, California.

Alvarez, J., J. Bair, D.H. Goodman, G. Hales, A. Hilton, S. McBain, A. Martin, and J. Polos. 2015(a). Integrated Habitat Assessment of the Upper Trinity River, 2009. U.S. Fish and Wildlife Service. Arcata Fish and Wildlife Office, Arcata Fisheries Technical Report Number TR 2015-28, Arcata, California.

Alvarez, J., D.H. Goodman, A. Martin, N.A. Som, K.A. Wright and T.B. Hardy. 2015(b). Development and validation of two-dimensional hydrodynamic models on the Trinity River, California. U.S. Fish and Wildlife Service. Arcata Fish and Wildlife Office, Arcata Fisheries Technical Report Number TR 2015-24, Arcata, California.

Aceituno, M.E., M. Gard, A. Hamilton, and M. Hampton. 1997. Physical Habitat Availability for Anadromous Salmonids in the Trinity River. U.S. Fish and Wildlife Service, Arcata Fish and Wildlife Office, Arcata, CA.

Bartley, R. and Rutherfurd, I. 2005. Measuring the reach-scale geomorphic diversity of streams: application to a stream disturbed by a sediment slug, *River Research and Applications* 21:39-59.

Beechie, T., G. Pess, and H. Imaki. 2012. Estimated changes to Chinook salmon (*Oncorhynchus tshawytscha*) and steelhead (*O. mykiss*) habitat carrying capacity from rehabilitation actions for the Trinity River, North Fork Trinity to Lewiston Dam.

Bisson, P.A., Nielson, J.L., Palmason, R.A., and Grove, L.E. 1982. A system of naming habitat types in small streams, with examples of habitat utilization by salmonids during low stream flow, In: *Acquisition and utilization of aquatic habitat inventory information*, Edited by N.B. Armantrout, American Fisheries Society, Bethesda, Md. pp. 62–73.

Boyce, J., D.H. Goodman, N.A. Som, J. Alvarez, and A. Martin. 2018. Trend Analysis of Salmon Rearing Habitat Restoration in the Trinity River at Summer Base Streamflow, 2005-2015. U.S. Fish and Wildlife Service.

Boyce, J., D.H. Goodman, N.A. Som, J. Alvarez, K. Hopkins, and A. Martin. 2020. Streamflow and Juvenile Salmonid Habitat Availability at Six Rehabilitation Sites on the Trinity River, California. Arcata Fisheries Technical Report TR2020-39 for the Trinity River Restoration Program (TRRP). U.S. Fish and Wildlife Service, Arcata, California.

Bradley, D. Nathan (2015). Trinity River 40 Mile Hydraulic Model: Development and Analysis, Technical Report No. SRH-2016-27, Prepared for Trinity River Restoration Program, August 2016.

Caldwell, T.J., G.J. Rossi, R.E. Henery, and S. Chandra. 2018. Decreased streamflow impacts fish movement and energetics through reductions to invertebrate drift body size and abundance. *River Research and Applications*. DOI: 10.1002/rra.3340.

CEFWG (California Environmental Flows Working Group). 2020. California Natural Flows Database: Functional flow metrics v1.1.0. November 2020. https://rivers.codefornature.org/. (Accessed December 2020).

Chamberlain, C.D., A.C. Martin, P.P. Petros. 2007. Trinity River Biological Monitoring of Channel Rehabilitation Sites: A Pre-construction Baseline habitat evaluation. U.S. Fish and Wildlife Service, Arcata Fish and Wildlife Office, Arcata Fisheries Technical Report TR 2007-07, Arcata, California.

De Juilio, K., A. Martin, J. Alvarez, and D.H. Goodman. 2014. Age-0 Chinook and Coho salmon rearing habitat assessment: Sawmill rehabilitation site, three years after construction at winter base flow, upper Trinity River. U.S. Fish and Wildlife Service. Arcata Fish and Wildlife Office, Arcata Fisheries Data Series Report Number DS 2014-37, Arcata, California.

DWR (Department of Water Resources). 2007. *Trinity River hydraulic flow study: North Fork Trinity to Lewiston Dam*. California Department of Water Resources, Sacramento, CA

Gaeuman, D., K. De Juilio, A. Martin, and D. Bandrowski. 2021. Sheridan Creek/Deep Gulch rehabilitation effectiveness monitoring report, WY2018-2020. Report for the Trinity River Restoration Program (TRRP). Yurok Fisheries Department, Trinity Division, Weaverville, California. Available: https://www.trrp.net/library/document?id=2484.

Gaeuman, D., A. Martin, and N.A. Som. 2019. Effect of increasing bed material storage on bed relief and rearing habitat in a reach of the Trinity River, California, *Proceedings of the Federal Interagency Sedimentation and Hydrologic Modeling Conference*, SEDHYD 2019, June 24-28, Reno NV.

Gaeuman, D., R. Stewart, and T. Buxton. 2016. First steps toward a river corridor management strategy, TRRP Technical Report TR-TRRP-2016-1, Trinity River Restoration Program, Weaverville, CA, https://www.trrp.net/library/document/?id=2294.

Gallagher, S.P. 1999(a). Use of Two-dimensional Hydrodynamic Modeling to Evaluate Channel Rehabilitation in the Trinity River, California, U.S.A. U. S. Fish and Wildlife Service, Arcata Fish and Wildlife Office, Arcata, CA. 36 pp.

Gallagher, S.P. 1999(b). Experimental Comparisons of Fish Habitat and Fish Use Between Channel Rehabilitation Sites and the Vegetation Encroached Channel of the Trinity River. U.S. Fish and Wildlife Service, Arcata Fish and Wildlife Office, Arcata, CA. 73 pp.

Goodman, D.H., A.M. Martin, J. Alvarez, A. Davis, and J. Polos. 2010. Assessing Trinity River salmonid habitat at channel rehabilitation sites, 2007-2008. United States Fish and

Wildlife Service, Arcata Fish and Wildlife Office, Yurok Tribe, and Hoopa Valley Tribe. Arcata Fisheries Technical Report Number TR 2010-13, Arcata, CA.

Goodman, D.H., J. Alvarez, A. Martin, N.A. Som, and J. Polos. 2012. Estimation of age-0 Chinook and coho salmon rearing habitat area within the restoration reach of the Trinity River at an index streamflow - Annual Report 2010. U.S. Fish and Wildlife Service. Arcata Fish and Wildlife Office, Arcata Fisheries Technical Report Number TR 2012-17, Arcata, California.

Goodman, D.H., N.A. Som, J. Alvarez, and A. Martin. 2014. A Mapping Technique to Evaluate Age-0 Salmon Habitat Response from Restoration. *Restoration Ecology*. doi:10.1111/rec.12148

Goodman, D.H., J. Alvarez, N.A. Som, A. Martin, and K. De Juilio. 2016. The Effects of Restoration on Salmon Rearing Habitats in the Restoration Reach of the Trinity River at an Index Streamflow, 2009 to 2013. U.S. Fish and Wildlife Service. Arcata Fish and Wildlife Office, Arcata Fisheries Technical Report Number TR 2016-25.

Gough, S. A., N. A. Som, K. Lindke, K. De Juilio, C. Laskodi, W. C. Matilton, and G. Kautsky. 2020. . U.S. Fish and Wildlife Service. Arcata Fish and Wildlife Office, Arcata Fisheries Synthesis Report Number TRRP-2020-011, Arcata, California.

Hawkins, C.P., J.L. Kershner, P.A. Bisson, M.D. Bryant, L.M. Decker, S.V. Gregory, D.A. McCullough, C. K. Overton, G.H. Reeves, R.J. Steedman, and M.K. Young. 1993. A Hierarchical Approach to Classifying Stream Habitat Features, *Fisheries* 18(6):3-12.

Hayes, J., E. Goodwin, K. Shearer, J. Hay, and L. Kelly. 2016. Can weighted useable area predict flow requirements of drift-feeding salmonids? comparison with a net rate of energy intake model incorporating drift-flow processes. *Transactions of the American Fisheries Society* 145: 589-609. 10.1080/00028487.2015.1121923.

Horan, D.L., J.L. Kershner, C.P. Hawkins, and T.A. Crowl. 2000. Effects of Habitat area and complexity on Colorado River cutthroat trout density in Uinta Mountain streams, *Transactions of the American Fisheries Society* 129:1250-1263.

Hampton, M. 1988. Development of Habitat Preference Criteria for Anadromous Salmonids of the Trinity River. U.S. Dept. Int., Fish Wildl. Serv., Div. Ecol. Serv. Sacramento, California. 93 pp.

Hampton, M. 1997. Microhabitat Suitability Criteria for Anadromous Salmonids of the Trinity River. U.S. Dept. Int., Fish Wildl. Serv., Div. Ecol. Serv. Sacramento, California.

HVT (Hoopa Valley Tribe) and McBain & Trush, Inc. 2012. Water Year 2010 Trinity River Restoration Program Geomorphic and Riparian Monitoring- A Sub-Component of the Integrated Habitat Assessment Project.

HVT (Hoopa Valley Tribe), Mcbain & Trush, Inc., Northern Hydrology & Engineering. 2011. Channel rehabilitation design guidelines for the mainstem Trinity River. Prepared for the Trinity River Restoration Program. Hoopa, CA.

Krause, A.F. 2012. *History of mechanical sediment augmentation and extraction on the Trinity River, California, 1912-2011*. TRRP Technical Report TR-TRRP-2012-2, Trinity River Restoration Program, Weaverville, CA.

Lane, B.A., H.E. Dahlke, G.B. Pasternack, S. Sandoval-Solis. 2017. Revealing the diversity of natural hydrologic regimes in California with relevance for environmental flows applications. *Journal of the American Water Resources Association* 53:411 – 430.

Lindke, K. 2020. Memorandum: Fish Work Group recommendation for programmatic use of Capacity habitat method. Prepared for James Lee, TRRP Science Coordinator. May 9, 2020.

Lisle, T.E. 1987. *Using `Residual Depths' to monitor pool depths independently of discharge*, USDA Pacific Southwest Forest and Range Experiment Station Research Note PSW-394, 4 pp.

Madej, M.A. 1999. Temporal and spatial variability in the thalweg profiles of a gravel-bed river, *Earth Surface Processes and Landforms* 24:1153-1169.

Martin, A., D.H. Goodman and J. Alvarez. 2012. Estimation of rearing habitat area for age-0 Chinook and coho salmon during winter base flows within the Sawmill Rehabilitation Site of the Upper Trinity River, 2010. Yurok Tribal Fisheries Program, Willow Creek, CA. U.S. Fish and Wildlife Service Arcata Fisheries Data Series Report Number DS 2012-26.

Martin, A., D.H. Goodman, and J. Alvarez. 2013. Age 0 Chinook and Coho Salmon Rearing Habitat Assessment of Lowden, Reading Creek, and Trinity House Gulch Rehabilitation Sites 2009-2011, Upper Trinity River. U.S. Fish and Wildlife Service. Arcata Fish and Wildlife Office, Arcata, California. Arcata Fisheries Data Series Number DS 2013-33.

McBain & Trush. 1997. Trinity River maintenance flow study final report. Prepared for Hoopa Valley Tribe Fisheries Department, Hoopa, CA. 482 pp.

Moffett, J.W., and S.E. Smith. 1950. Biological Investigations of the Fishery Resources of Trinity River, California. *Special Scientific Report: Fisheries No. 12*. www.krisweb.com/biblio/trinity_usfws_moffett_1950.pdf

Naman, S.M., J.S. Rosenfeld, J.R. Neuswanger, E.C. Enders, and B.C. Eaton. 2019. Comparing correlative and bioenergetics-based habitat suitability models for drift-feeding fishes. Freshwater Biology. DOI: 10.1111/fwb.13358.

Olden, J.D. and R.J. Naiman. 2009. Incorporating thermal regimes into environmental flows assessments: modifying dam operations to restore freshwater ecosystem integrity. *Freshwater Biology* 55: 86-107.

Perry, R.W., J.M. Plumb, E.C. Jones, N.A. Som, N.J. Hetrick, N.J., and T.B. Hardy. 2018a. Model structure of the stream salmonid simulator (S3)—A dynamic model for simulating growth, movement, and survival of juvenile salmonids: U.S. Geological Survey Open-File Report 2018-1056, 32 p., https://doi.org/10.3133/ofr20181056.

Perry, R.W., E.C. Jones, J.M. Plumb, N.A. Som, N.J. Hetrick, T.B. Hardy, J.C. Polos, A.C. Martin, J.S. Alvarez, and K.P. De Juilio. 2018b. Application of the Stream Salmonid Simulator (S3) to the restoration reach of the Trinity River, California—Parameterization and calibration: U.S. Geological Survey Open-File Report 2018-1174, 64 p., https://doi.org/10.3133/ofr20181174.

Petty, J. T., D. Thorne, B. M. Huntsman, and P. M. Mazik. The temperature-productivity squeeze: constraints on brook trout growth along an Appalachian river continuum. *Hydrobiologia* 727: 151-166.

Pinnix, W.D., K. De Juilio, P. Petros, and N.A. Som. 2016. Feasibility of Snorkel Surveys for Determining Relative Abundance and Habitat Associations of Juvenile Chinook Salmon on the Mainstem Trinity River, California. Yurok Tribal Fisheries Program, Hoopa Valley Tribal Fisheries Department, U. S. Fish and Wildlife Service, Arcata Fish and Wildlife Office, Arcata Fisheries Technical Series Report Number TR 2016-24, Arcata, California.

Pinnix, W.D., D. Rupert, N.A. Som, P. Petros, and K. DeJuilio 2019. The Use of Small 2-Dimensional Habitat Zones and Dual-Snorkeler Surveys to Model the Habitat Use of Juvenile Salmonids in the Trinity River, California. U.S. Fish and Wildlife Service. Arcata Fish and Wildlife Office, Arcata Fisheries Technical Report Number TR 201937, Arcata, California.

R Core Team (2019). R: A language and environment for statistical computing. R Foundation for Statistical Computing, Vienna, Austria. URL https://www.R-project.org/.

Rayburg, S.C. and M. Neave. 2008. Assessing morphologic complexity and diversity in river systems using three-dimensional asymmetry indices for bed elements, bedforms and bar units, *River Research and Applications* 24:1343-1361.

Rosenfeld, J. and R. Ptolemy. 2012. Modelling available habitat versus available energy flux: do PHABSIM applications that neglect prey abundance underestimate optimal flows for juvenile salmonids? *Canadian Journal of Fisheries and Aquatic Sciences* 69: 1920-1934.

Som, N.A., R.W. Perry, E.C. Jones, K. De Juilio, P. Petros, W.D. Pinnix, and D.L. Rupert. 2018. N-Mix for Fish: Estimating Riverine Salmonid Habitat Selection via N-mixture Models. *Can. J. Fish. Aquat. Sci.* **75:** 1048-1058

Sullivan, K., D.J. Martin, R.D. Cardwell, J.E. toll, and S.Duke. 2000. An analysis of the effects of temperature on salmonids of the Pacific Northwest with implications for selecting temperature criteria. Sustainable Ecosystems Institute, Portland, OR.

Trainor, K. and M. Church. 2003. Quantifying variability in stream channel morphology, Water Resources Research 39(9), 1248, doi:10.1029/2003WR001971.

TRRP and ESSA Technologies Ltd. 2009. *Integrated Assessment Plan, Version 1.0 – September 2009*, Report prepared for the Trinity River Restoration Program, Weaverville, CA. 285 pp, https://www.trrp.net/library/document/?id=400.

Yarnell S.M., J.F. Mount, and E.W. Larsen. 2006. The influence of relative sediment supply on riverine habitat heterogeneity, *Geomorphology* 80:310-324.

Yarnell S.M., G.E. Petts, J.C. Schmidt, A.A. Whipple, E.E. Beller, C.N. Dahm, P. Goodwin, J.H. Viers JH. 2015. Functional Flows in Modified Riverscapes: Hydrographs, Habitats and Opportunities. *BioScience* 65:10:963–972. https://doi.org/10.1093/biosci/biv102

USBR. 1970. Sacramento, California Regional Director memo to Commissioner Washington D. C.: Fish Habitat Characteristics of Trinity River. April 24, 1970.

USBR (United States Bureau of Reclamation). 1984. *Trinity River Fish Hatchery Modification Program, Final Report*. Mid-Pacific Region, Sacramento, CA, https://www.trrp.net/library/data/?id=1888.

USDI (U.S. Department of Interior). 2000. Record of Decision, Trinity River mainstem fishery restoration final environmental impact statement/environmental impact report. U.S. Department of Interior, Washington D.C.

USFWS (United States Fish and Wildlife Service) and CDFG (California Department of Fish and Game). 1956. "A plan for the protection of fish and wildlife resources affected by the Trintiy River Division, Central Valley Project." 76 pp.

USFWS (United States Fish and Wildlife Service). 1989. *Trinity River Flow Evaluation, Annual Report – 1989*. USFWS, Sacramento Field Office, Sacramento, CA, https://www.trrp.net/library/data/?id=501.

USFWS (United States Fish and Wildlife Service) and HVT (Hoopa Valley Tribe). 1999. Trinity River Flow Evaluation Final Report. U.S. Fish and Wildlife Service, Arcata Fish and Wildlife Office, Arcata, CA and Hoopa, CA.

USHR (United States House of Representatives). 1955. 84th Congress, 1st session, Report No. 602 ct. Authorizing the Secretary on the Interior to construct, operate, and maintain the Trinity River Division, Central Valley Project, California, under federal reclamation laws.

Weber, N., N. Bouwes, C.E. Jordan. 2014. Estimation of salmonid habitat growth potential through measurements of invertebrate food abundance and temperature. *Canadian Journal of Fisheries and Aquatic Sciences* 71(8): 1158-1170. https://doi.org/10.1139/cjfas-2013-0390

Wheaton, J.M., N. Bouwes, P. Mchugh, C. Saunders, S. Bangen, P. Bailey, M. Nahorniak, E. Wall, and C. Jordan. 2017. Upscaling site-scale ecohydraulic models to inform salmonid

population-level life cycle modeling and restoration actions – lessons from the Columbia River Basin. *Earth Surface Processes and Landforms*. DOI: 10.1002/esp.4137

Yurok Tribe. 2021. *Revised 90% design report, Trinity River rehabilitation site at Oregon Gulch*. Report to the Trinity River Restoration Program, Weaverville, CA.